VALIDATING SUB-SEA GAS PIPELINE LEAKS DISCHARGE MODEL FOR ARABIAN SEA CONDITIONS
by
P.C.Sridher,
SAP ID-500010363

COLLEGE OF ENGINEERING

Submitted

Harnessing Energy through Knowledge

IN PARTIAL FULFILLMENT OF THE REQUIREMENT
OF
THE DEGREE OF DOCTOR OF PHILOSOPHY
to
UNIVERSITY OF PETROLEUM & ENERGY STUDIES
DEHRADUN
20th Sep, 2013

Centre for Continuing Education | University of Petroleum & Energy Studies

<u>THESIS COMPLETION CERTIFICATE</u>

This is to certify that the thesis on '**VALIDATING SUB-SEA GAS PIPELINE LEAKS DISCHARGE MODEL FOR ARABIAN SEA CONDITIONS'** by **P.C.SRIDHER, SAP ID-500010363** in Partial completion of the requirements for the award of the Degree of Doctor of Philosophy (Engineering) is an original work carried out by him under our joint supervision and guidance.

It is certified that the work has not been submitted anywhere else for the award of any other diploma or degree of this or any other University.

External Guides

Name   **: Dr. Vijaya Baskher Reddy**

Signature   :

Internal Guide:

Name   : **Dr. Shrihari**

Signature   :

REVISION HISTORY

Rev	Description	Date
0.0	'Initial Draft' prepared with the assistance of External Guide	21.08.2011
1.0	'Research methodology' chapter was thoroughly reviewed and updated based on comments by Internal Guide	28.12.2012
2.0	The final results of IIT experimentation were incorporated	10.04.2012
3.0	Comments from Faculty Research Committee (FRC) were incorporated. Experimentation graphs were updated using polynomial curve fittings	04.07.2012
4.0	Comments from the Evaluators were incorporated, mainly the results from experimentation were validated using CFD modelling	20.09.2013

EVALUATION

Name of Faculty 1	Date	Signature	Remarks

Outstanding _____

Good _____

Satisfactory _____

Meets minimum standards _____

Unsatisfactory _____

Name of Faculty 2	Date	Signature	Remarks

Outstanding _____

Good _____

Satisfactory _____

Meets minimum standards _____

Unsatisfactory _____

ACKNOWLEDGEMENTS

The satisfaction and elation that accompany the completion of my Dissertation would be incomplete without the mention of the people who have made it a possibility. It is a great privilege to express my gratitude and respect to all those who have guided me and inspired me during the course of my research work.

First and foremost, I would like to express my sincere gratitude to my Research Guides Dr. Shrihari, the Dean, Centre for Continuing Education (CCE), UPES and Dr. Vijaya Baskher Reddy of Abu Dhabi Company for On-shore Oil Operations (ADCO), Abu Dhabi for their constant guidance and supervision during the period of my research work. Without their generous help and expert advice, I would not have been able to pursue my research into this rather uncharted topic.

My most sincere and heartfelt thanks to Dr.S.Bhattacharya, Head of Ocean Eng. Dept., IIT-Madras and to Mr.M.Santhanam, Technical Officer for their valuable guidance and support in carrying out the experimentation in their world-class research laboratory.

My sincere thanks are due to Mr. Rajneesh Kumar, Head of Operations and Mr. R.Krishnan, Principal Process Engineer of M/s International Risk Control Asia (IRCA), the leading international safety consultancy firm in the field of Oil and Gas for sharing pertinent technical information for my research work.

Last, but not the least, I would like to thank my colleagues, my friends and family for their steady stream of encouragement and unwavering support. It was their shadow during my most testing and doubtful moments that gave me the impetus to forge ahead with my research work.

ABSTRACT

The field of consequence modelling for hydrocarbon releases in open atmospheric conditions is highly developed, and there are several commercially available computer programs to model the discharge, dispersion and fire/explosion effects of gases and liquids. Some of these techniques are relatively simple, and are suitable for manual analysis, and have commonly been implemented in customized spread sheets. More complex models are available in stand-alone format and also as part of linked software or toolkits.

The study of sub-sea gas pipeline leaks plume behavior is very vital from the risk assessment point of view. In the recent years some research works were done in UK and Norway to study the sub-sea gas leaks plume behaviour for North Sea and Norwegian Sea conditions (< 500 m depth). However as of now no such research work is carried out anywhere for Arabian Sea Conditions for higher depths ranging 500 m to 1500 m.

This paper analyses various sub-sea gas discharge models used in North Sea and Norwegian Sea namely:

a. The E*mpirical models* that assume the plume radius is proportional to the release depth or correlations that have been produced to fit the available experimental data.

b. *Integral models* that are based on local similarity i.e. the radial profiles of velocity and density defect are assumed to have a similar form at different heights within the plume. The plume properties are represented using Gaussian profiles by their plume centreline values.

c. The *Computational Fluid Dynamics (CFD)* or field codes that solve the Navier Stokes equations of fluid flow.

Striking a right balance between accuracy, uncertainty, cost effectiveness and user-friendliness, clearly, the simple empirical 'model' remains most favoured for use in risk assessments.

In this thesis, the Empirical gas discharge model established in North Sea and Norwegian Sea (for depths < 500 m) was validated for Arabian Sea conditions (higher depths ranging from 500m to 1500 m) through lab-scale experimentation and CFD modelling.

The outcome of this research will help in ascertaining the accuracy of safety sensitive studies and consequence analysis of the sub-sea gas pipelines leaks for Arabian Sea Conditions i.e. higher Sea depths ranging from 500 m to 1500 m.

EXECUTIVE SUMMARY

A number of Gas leaks from subsea pipelines have been recorded in recent years. These occurrences highlight the need for better understanding of the way Gas leaks (plume) behave under water and the risks they present. The effects of subsea hydrocarbon release depend on a number of factors, including whether the release is liquid or gas.

a. For a liquid release, the buoyancy will result in the leaked material spreading on the surface to form either a polluting slick, or an expanding pool fire.

b. For a gas release, although the buoyancy is rather greater, significant drag forces will cause the plume to break up and rise to the surface as a series of bubbles. On breaking surface, ignition of the gas plume would result in a sea surface fire with different characteristics to those incorporated into the usual pool and jet fire models.

c. Alternatively, and more likely, the plume will begin to disperse in the atmosphere, and may be diluted to a concentration below the lower flammable limit before there is any possibility of encountering an ignition source.

d. A further effect of a gas bubble plume is the reduction in the stability of floating vessels, due to either the loss of buoyancy, or, more likely, due to the radial outflow of water which has been entrained into the plume.

Consequence models are used to predict the physical behaviour of hazardous incidents mainly flammable and toxic releases. Some models only calculate the effect of a limited number of physical processes, like discharge or radiation effects. More complex models interlink the various steps in consequence modelling into one package. The field of consequence modelling for hydrocarbon releases in open atmospheric conditions is highly developed. *Whereas, the understanding about the behaviour of a subsea gas release up through the water column (plume raise) is very limited from risk assessment point of view.* The hydrodynamic basis for bubble-plume flows is reasonably well understood, but the solutions of the associated equations, depend on a large number of parameters that can only be evaluated by experimentation.

In the recent years some research works were carried out in UK and Norway to study the subsea gas leaks plume behaviour for North Sea and Norwegian Sea conditions.

The discharge of the gas from the release point to the surface is considered in three zones.

Zone of Flow Establishment (ZOFE): The region between the release point and the height at which the dispersion appears to adopt a plume-like structure. At this height the effects of initial release momentum are considered to be secondary to the momentum induced by buoyancy.

Zone of Established Flow (ZOEF): The plume-like region of dispersion which extends from the ZOFE to a depth beneath the free surface which is of the order of one plume diameter.

Zone of Surface Flow (ZOSF): The region above the ZOEF where the plume interacts with the surface causing widening of the bubble plume and radial flow of water at the surface.

Three approaches, of varying complexity, have been used in modelling the discharge of subsea releases in North Sea and Norwegian Sea:
   a. Empirical/ Cone model
   b. Integral Model
   c. Computational Fluid Dynamic (CFD) model

The simplest are *empirical models* which consist of those that assume the plume radius to be proportional to the release depth or correlations that have been produced to fit the available experimental data.

Integral models are based on local similarity i.e. the radial profiles of velocity and density defect are assumed to have a similar form at different heights within the plume. The plume properties can be represented, using for example *Gaussian profiles,* by their plume centreline values. Entrainment of water into the plume is described using a correlation relating the rate of increase of water flow to the plume centreline properties through the use of an entrainment coefficient, as is used in single phase plume modelling. Gas continuity, and equating the increase in momentum to the buoyancy forces, allows the plume properties to be calculated in a step-by-step manner as the height above the release is incremented. Separate models have been produced for the ZOEF and the ZOSF as described in integral models for initial release and integral models for the region of established flow respectively.

The most complex models are represented by *Computational Fluid Dynamics (CFD)* or field codes which solve the Navier Stokes equations of fluid flow. Their advantage over integral models is that effects such as entrainment and turbulent transport of momentum are modelled directly and do not require the use of empirical constants. However, they still involve some

modelling assumptions, as described in CFD models, and are more resource-intensive to run than integral or empirical models.

Striking a right balance between accuracy, uncertainty, cost effectiveness and user-friendliness, clearly, the simple empirical 'model' remains most favoured for use in risk assessments.

The objectives of this thesis are:
   a. To identify various sub-sea gas discharge models that are currently being used in North Sea and Norwegian Sea with respect to plume discharge (initial release of plume to the sea surface from the point of leak);
   b. To study and analyse the accuracy and uncertainty levels of various discharge models used in North Sea and Norwegian Sea based on the feedback received from lab scale experimentation and limited filed trials carried out so far;
   c. Identify the most optimal discharge model suitable for Arabian Sea conditions striking a right balance between i) accuracy, ii) uncertainty, iii) cost-effectiveness and iv) user-friendliness;
   d. Validate the chosen model for Arabian Sea Conditions based on lab-scale experimentation and CFD Modelling.

In this study the available information on the bubble plumes, both theory and experiments was reviewed for the purpose of improving our prediction capabilities of small to medium releases which are common.

Lab-scale experimentation was held at Department of Ocean Engineering, Indian Institute of Technology (IIT), Madras for validating the Empirical/ Cone gas discharge plume models established in North Sea & Norwegian Sea for Arabian Sea conditions. The main parameters considered for experimentation were release rate, gas density, and depth of release, sea temperature and salinity. The results of IIT experimentation were corroborated using CFD modelling.

In conclusion, the plume model established through IIT experimentation for Arabian Sea conditions very well matches with the Plume model established by Fanneløp and Sjøen (1980) [7] and the plume measurements published by Milgram (1983) [17] for North Sea and Norwegian Sea conditions.

CONTENTS

LIST OF FIGURES

LIST OF TABLES

1. INTRODUCTION

1.1 Chapter Overview

This chapter contains various definitions used in this thesis; details research motivation, an overview of research model, research approach, contribution of this research to Oil and Gas industry operating in Arabian Sea, and outline of thesis chapters.

1.2 Definitions

1.2.1 Bubble Slip Velocity

The difference in velocities between liquids and solids (or gases and liquids) in the vertical flow of two phase mixtures through a pipe because of slip between two phases.

1.2.2 Centreline velocity

It is defined as the distance measure from the centreline of the jet where the local mean velocity is equal to half of the local centreline mean velocity.

1.2.3 Computational Fluid Dynamics (CFD)

CFD is a branch of fluid mechanics that uses numerical methods and algorithms to solve and analyze problems that involve fluid flows. Computers are used to perform the calculations required to simulate the interaction of liquids and gases with surfaces defined by boundary conditions.

1.2.4 Consequence Analysis

Consequence analysis quantifies vulnerable zone for a conceived incident.

1.2.5 Consequence Analysis modelling

Consequence Analysis Modelling is the generation of a toxic and/or flammable vapour cloud from a release source and profiling the possible toxic, flammable, and explosion hazard zones.

1.2.6 Discharge

Discharge is defined as the release of gas/ air under liquid.

1.2.7 Dispersion

Dispersion is defined as the release of gas in open atmosphere.

1.2.8 Entrainment coefficient

The ratio of lateral (entrainment) velocity to plume-rise velocity of plume is the entrainment coefficient α. Plumes that rise due to buoyancy or momentum become diluted with surrounding fluid, where the rate of dilution is proportional to the rise rate of the plume. The entrainment coefficient is this constant of proportionality.

1.2.9 Flow rate/ release rate

Volumetric flow rate is the volume of fluid which passes through a given surface per unit time. SI Unit for flow rate is m^3/ sec.

1.2.10 Hazard

Hazard is the potential to cause harm to People, Environment, Asset and Reputation (PEAR) of an organisation.

1.2.11 Hydrodynamics

Hydrodynamics is the study of dynamics of fluids in motion or the scientific study of the motion of fluids, under the influence of internal and external forces.

1.2.12 Individual Risk Per Annum (IRPA)

Individual Risk Per Annum is the chance of an individual becoming a fatality. An IRPA of 1 x 10^{-3} would mean for each individual, every year, there is a 1 in 1000 chance of a fatal accident.

1.2.13 Momentum Amplification Factor

The momentum amplification factor ϒ is defined as the ratio of total momentum flux to the momentum flux carried by mean flow and is a measure for the momentum flux due to turbulent fluctuations. Large values of this parameter are found in small-scale laboratory experiments. This is the case also for the phenomenon known as plume wandering. As the bubbles become very small in comparison with the plume dimensions, bubble dynamics and interactions become less important and the flow behaves like a single-phase fluid.

1.2.14 Potential Loss of Life (PLL)

Potential Loss of Life is proportional to the sum of all the IRPAs. In simple terms PLL is related to IRPA by the relationship IRPA = PLL x fraction of time an individual is present on offshore per year.

1.2.15 Plume

A structure or form that is like a mushroom or ice cream cone: a plume of subsea gas discharge.

1.2.16 Plume density

Plume density is the mass of plume gases per unit volume. The SI unit is kg/m^3

1.2.17 Plume width (Gaussian shape)

Plume width defined as point where concentration drops to 10% of centerline value (± 2.15 σ)

-2.15 σ -2 σ   -1 σ   +1 σ   +2 σ +2.15 σ

Plume width = 4.3 σ
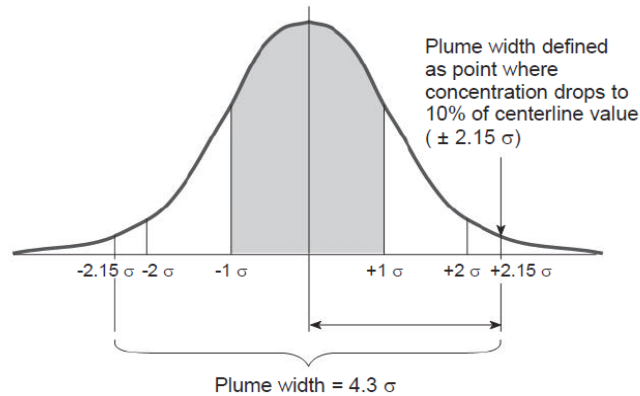
1.2.18 Quantitative Risk Assessment (QRA)

Quantitative risk assessment (QRA) is a formal systemized approach for hazards identification and ranking. The final rating number provides a relative ranking of the hazards. Fire and Explosion Index (F and EI) is an important technique employed for hazards identification process. Consequence analysis then quantifies the vulnerable zone for a conceived incident.

1.2.19 Risk

Risk = Hazard Potential (Consequence) x Frequency of incident happening (failure).

1.2.20 Salinity

Salinity is the saltiness or dissolved salt contents (sodium chloride, magnesium, calcium sulphates and bi-carbonates) of the body of water.

1.2.21 Temperature

Temperature is a measurement of the average kinetic energy of the molecules in an object or system and can be measured with a thermometer or a calorimeter. It is a means of determining the internal energy contained within the system.

1.2.22 Void fraction

Void fraction is a measure of the void (i.e., "empty") spaces in a plume, and is a fraction of the volume of voids over the total volume, between 0–1, or as a percentage between 0–100%.

1.2.23 Width Ratio

The length-to-width ratio is a comparison of the length and the width of a plume. The range of variation in λ is smaller and the effect on the plume development is much less important. The lower values correspond also to laboratory experiments, whereas for very large scales λ is expected to approach unity.

1.3 Abbreviations

CFD	Computational Fluid Dynamics
DPM	Discrete Phase Model
E&P	Exploration & Production
ESD	Emergency Shut Down
F and EI	Fire and Explosion Index
HSE	Health and Safety Executive, UK
IIT	Indian Institute of Technology, Madras
IRPA	Individual Risk Per Annum
LCWM	Long Crested Waves Maker
MEWM	Multi-Element Wave Maker
NIOT	National Institute of Ocean Technology
NOAA	National Oceanic and Atmospheric Administration
PEAR	People, Environment, Asset and Reputation
PIV	Particle Image Velocimetry
PLL	Potential Loss of Life
PSA	Petroleum Safety Authority
QRA	Quantitative risk assessment
USCG	US Coast Guard
VOF	Volume of Fluid
ZOEF	Zone of Established Flow
ZOFE	Zone of Flow Establishment
ZOSF	Zone of Surface Flow

1.4 Research motivation

A number of incidents involving hydrocarbon leaks from wells, subsea installations and pipelines have been recorded in recent years like submarine gas blowout on the Snorre, an offshore installation in 2004 and like the ones that are listed below. While the understanding of atmospheric gas dispersion is far advanced, *the need for better understanding of the way hydrocarbon emissions (Plume) behave under water and the risks they present need to greatly improve.* Though limited research is done in UK and in Norway to study the plume behavior for North Sea and Norwegian Sea conditions (< 400 m depth), no such research is done so far in Arabian Sea (for depths ranging from 500m to 1500 m). As the deep water Oil and Gas Exploration and Production will be actively pursued in near future, the need to study the deep-set plume is very essential and hence this research.

Some of the sub-sea gas pipeline leaks reported in this decade is listed below. Ref. Jan Erik Vinnem, 2007 [11].

April 29, 2001

Texaco Exploration and Production Pipeline segment no. 10393

South Marsh Island, Block 236 Water Depth: 14 feet

An incoming 2-inch gas lift line was ruptured. The break caused damage to the upper work deck, handrails, flow line, and riser. The line appeared to have been pulled from the structure prior to the rupture possibly by a shrimp vessel since the line was buried. Personnel working on an adjacent well heard the bleeding gas, reported the incident to Texaco personnel who immediately shut-off the supply of gas to the line. No injuries or pollution were reported.

January 3, 2002

Chevron USA Inc. Pipeline segment no. 13154

West Cameron, Block 48 Water Depth: 22 feet

During an ESD shut-in, the 10-inch incoming shutdown valve closed, but the safety system on the platform failed to operate. Shortly after, the platform operators noticed gas bubbles in the water approximately 300 feet from the platform. The pipeline, which was 37 years old, was allowed to bleed for 90 minutes, and was later found to have ruptured in three places. It appears that the safety system failure was due to freezing problems in the ¼-inch tubing, which runs approximately 40 feet to the transmitter.

January 15, 2002

Transcontinental Gas Pipeline Company Pipeline segment no. 1526

Vermillion, Block 67 Water Depth: 40 feet

The operator at an adjacent platform reported a pipeline rupture with a fire on the water, located ½ to ¾ miles west of their location. Within 2 hours Transco confirmed it was their pipeline, a 16- inch gas pipeline. The pipeline was shut-in and the fire ceased. No injuries or pollution were reported.

July 6, 2002

ChevronTexaco Corporation Pipeline segment no. 3540

South Marsh Island, Block 217 Water Depth: 15 feet

The pipeline was reported as having ruptured, with the ensuing fire having flames 100 feet high. The location of the rupture was 6000 feet north of SM 217 A. The flames lasted for 2 hours. The pipeline PSL got shut-in the platform at the time of the rupture.

January 7, 2003

Walter Oil and Gas Corporation Pipeline segment no. 11052

South Timbalier, Block 260 Water Depth: 303 feet

A vessel moored 2.2 miles from the platform snagged the associated gas pipeline while retrieving its anchor. The vessel began pulling up the anchor and halted the operation an hour later when the Captain realized he had snagged a heavy object. Ten minutes later, the Captain noticed fire and smoke under the platform and notified the USCG. Subsequently, the platform operator felt several jolts to the platform that intensified in strength and eventually rocked the platform. The operator shut-in the platform's two producing wells. About 10 minutes later, the platform was jolted again: the gas pipeline broke loose and an explosion and fire erupted from the severed pipeline beneath the platform. The three individuals on the platform at the time evacuated the facility via helicopter. The vessel had been moored outside of the designated lightering area per the instructions of the Mooring Master. The Mooring Master and the Captain were unaware of any pipelines in the mooring area as apparently neither one had a copy of the pipeline overlay to the NOAA nautical chart.

December 2, 2003

South Pipeline Company, LP Pipeline segment no. 5105

Eugene Island, Block 39 Water Depth: 10 feet

A dredge barge, dredging the Atchafalaya Channel for the Corp of Engineers, impacted and severed the 20-inch gas pipeline. The barge was dredging the channel floor to a depth of 22 feet BML in the vicinity of the pipeline; however, the burial depth of the pipeline was not known. A representative of the pipeline company was not on board at the time of incident. The project engineer did not account for the length of the dredge (420 feet) in determining where to halt dredging operations relative to the location of the pipeline. The pipeline caught on fire as a result of the impact from the dredge. Approximately 1,500 feet of pipe was pulled apart or ripped.

Fig 1.1 Hydrocarbon leaks > 0.1Kg/s, Norwegian sector Ref. Jan Erik Vinnem, 2007 [11]
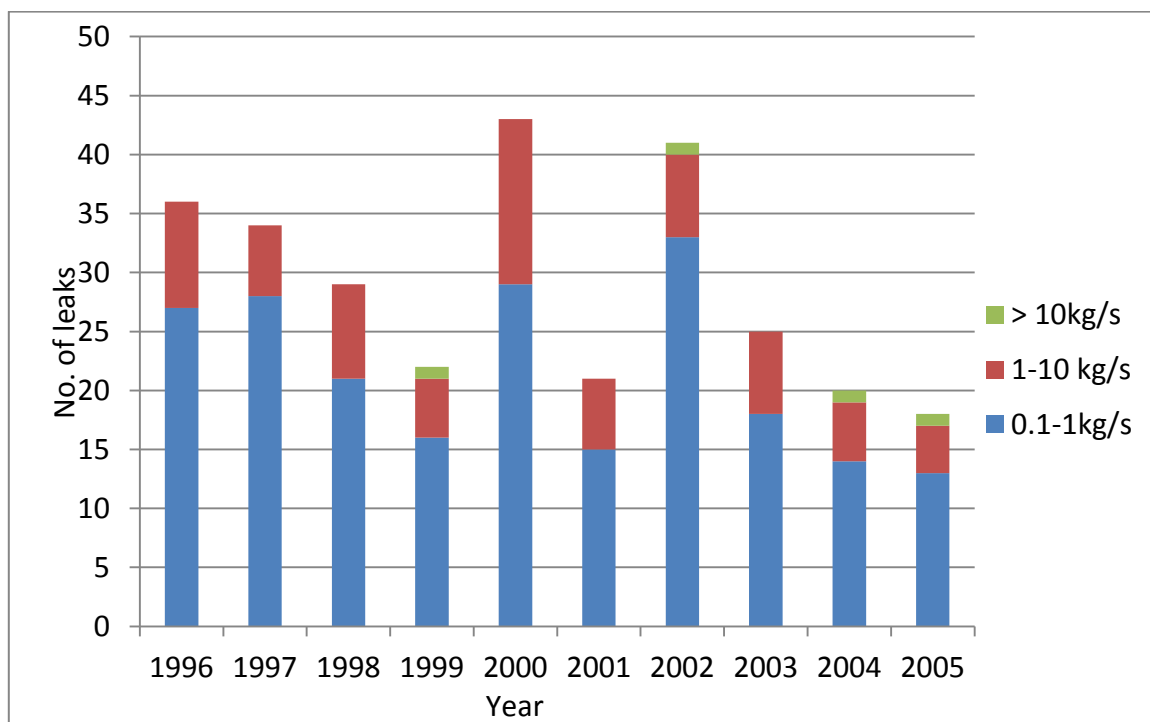
1.5 An overview of research model

The analysis of the consequences of hydrocarbon releases involves several stages, from release rate and associated depressurization calculations, through the modelling of liquid spread and gas dispersion, to the assessment of the effects of fire and explosion, and their potential for escalation. *For subsea hydrocarbon releases, there is an additional intermediate stage (Discharge) to be considered linking the release rate from the Leak position to the Sea surface* prior to a gas dispersion model or fire model at the sea surface. This intermediate stage (Plume discharge modelling) is the subject of the study reported here.
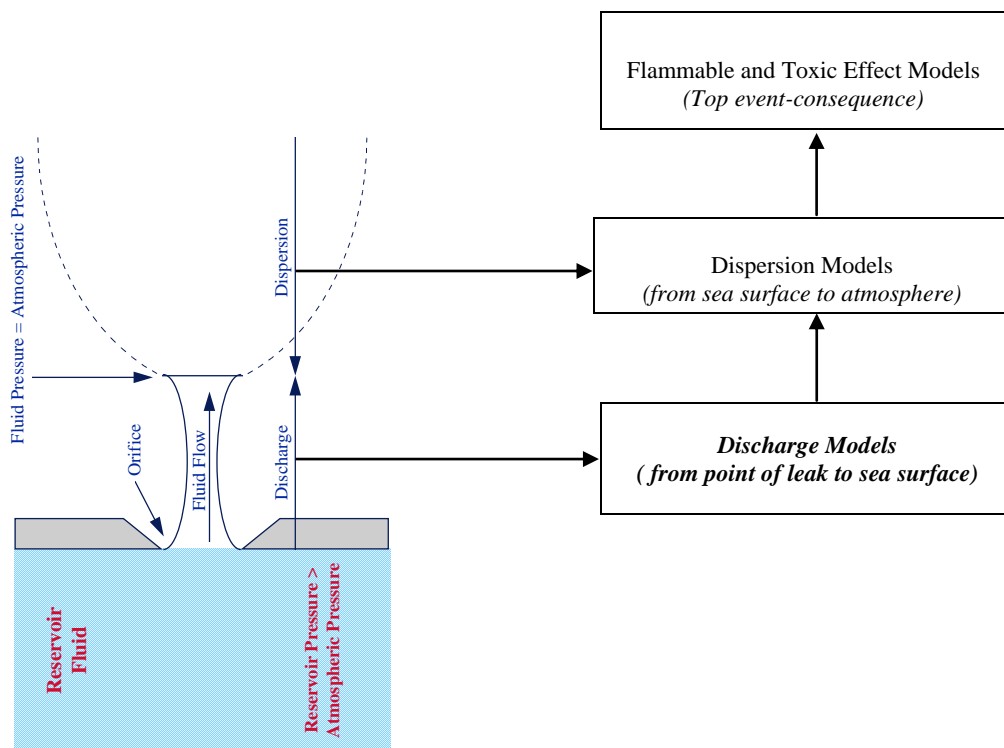
Fig 1.2 Gas discharge model

1.6 Overview of research approach

INPUT *(Literature survey)*	PROCESS *(Lab-scale Experimentation & CFD Modelling)*	OUTPUT *(Validated model for Arabian Sea Conditions)*
Identify and Study various discharge models that are currently being used in North Sea and Norwegian Sea with respect to plume discharge from Consequence point of view. Identify the optimal gas discharge (plume raise) model that best suits Arabian Sea conditions	Validate the identified model for Arabian Sea conditions by lab-scale experimentation AND Corroborate the results of experimentation with CFD modelling	Cost effective, reliable, user-friendly Sub-Sea Gas dispersion model that is tested and validated for Arabian Sea Conditions

1.7 Contribution of this research

In Oil and Gas industry, safety sensitivity studies are undertaken at two levels, relating respectively to consequence modelling and risk assessment. *For consequence modelling, typical release rates and water depths are identified, and, for typical values of these parameters, the above sea consequences are evaluated* for and range of assumptions concerning the interface between the subsea bubble plume and the surface plume or fire.

In the recent past, several lab-scale studies were carried out in UK and Norway for modelling the sub-sea gas pipelines leak plumes for North Sea and Norwegian Sea conditions i.e. for typical depths ranging from 100 m to 400 m. As an outcome of these studies, several plume discharge models were established. Out of all, the Empirical/Cone model established by Wilson (1988) [25] and Milgram and Erb (1984) is found to be fairly an accurate, economical and preferred model for practical application in industrial safety sensitive studies.

The purpose of this research is to test and validate the Empirical/Cone model established by Wilson (1988) [25] and Milgram and Erb (1984) for Arabian Sea conditions i.e. higher Sea depths ranging from 500 m to 1500 m.

1.8 Outline of Thesis chapters:

Chapter No.	Chapters	Chapter Outline
1	Introduction	This chapter contains various definitions used in this thesis; details research motivation, an overview of research model, overview of research approach, contribution of this research to Oil and Gas industry operating in Arabian Sea, and outline of thesis chapters.
2	Literature survey	This chapter lists chronological order of research done worldwide, researcher (s) and contribution. Identifies the most popular discharge models that are currently being used in North Sea and Norwegian Sea. Analyses the merits and demerits of the most popular models used in North Sea and Norwegian Sea, and suggests the best suited model for Arabian Sea conditions.
3	Research Problem	This chapter introduces the research problem, highlights the implications of the research problem and the influence of research problem on offshore Exploration and Production companies operating in Arabian Sea.
4	Research Methodology	This chapter outlines the objectives of this research, methods and materials involved. It outlines the sub-sea gas bubble plume calculation basis, usage of past experimentation results, uncertainty of past experimentation, scale refinement, algorithms used for IIT experimentation, and the limitations.

5	Experimentation	This chapter details the experimental set up at IIT, experimentation parameters, experiential readings, data mining methods used to refine raw data, key finding and conclusions of lab scale experimentation.
6	Models for research problem's competence	This chapter compares and analyses in details, the empirical plume model established through IIT Experimentation for Arabian Sea conditions with the empirical plume model established in North Sea and Norwegian Sea. The outcome of CFD modelling carried out to corroborate the results of IIT experimentation is also included in this chapter.
7	Conclusions and future research	This chapter covers the summary of conclusions of this thesis and the scope for further research.

2. LITERATURE SURVEY

2.1 Chapter overview

This chapter lists chronological order of research done worldwide, researcher (s) and contribution, analyses in details, the Subsea gas discharge models established in UK and Norway for North Sea and Norwegian Sea conditions [22].

2.2 Chronological order of research done and researcher(s) and contribution

Table 2.1 Research done and researcher (s) and contribution

Order	Name of Researcher	Area of Research done
1	Ditmars and Cederwall (1974)	The work of Ditmars and Cederwall pre-dates that of Milgram, and differs in a number of respects. Firstly, they invoke the Boussinesq assumption to simplify the momentum equation, such that the mean density of the mixture of gas and fluid is identical to that of the fluid alone. This difference in density is of course retained for the generation of buoyancy forces. Secondly, no account is taken of the increase in momentum flux due to transport by turbulent fluctuations. [4].
2	Mc Dougal (1978)	Mc Dougal (1978) extended the model developed by Ditmars and Cederwall (1974) to include the effect of a release in a stratified environment. [13].
3	Peng Robinson equation of state, (1976)	A compositional model is used to predict the hydrocarbon phase behavior and thermo-dynamical properties. The calculations are based on the concept of an equilibrium constant, K value, defined as the ratio of the mole fraction of the component in the gas phase, to the mole fraction of the same component in the liquid phase. Unlike a single component fluid, a multi component mixture exhibits a phase envelope rather than a single equilibrium curve. This implies that pressures and temperatures inside the phase envelope, both liquid and gas phases exists in equilibrium. [21].

		The Peng-Robinson equation is expressible in terms of the critical properties and the acentric factor. The equation is applicable to calculations of fluid properties in natural gas processes and is expected to provide good accuracy for the scenarios intended for the release model.
4	Scorer (1978)	Developed Zone of formation model for calculating mean gas concentration above an underwater release (plumes with excess of buoyancy).
5	Fazal and Milgram (1980)	Developed an integral formulation which assumes the mean fluid velocity and mean density defect within the plume are assumed to take the form of Gaussian distributions. [8]
6	Fannelop and Sjoen (1980)	Fannelop and Sjoen (1980) again proceeding Milgram (1983) developed a model based upon the work of Ditmars and Cederwall (1970) [3]. However a number of differences exist in the representation of buoyancy, the inclusion of the bubble slip velocity, and the use of top-hat as well as Gaussian velocity profiles. [7]
7	Milgram and Van Houten (1982)	The Milgram model for the Zone of Established Flow (ZOEF) was also used by Milgram and Van Houten (1982) in a paper which again compared experiments at small scale with computed data, and presented the results of large scale calculations. [16]
8	Milgram (1983)	Produced data related to empirical correlations for the plume diameter and the gas velocity.[17]
9	Milgram and Burgees (1984)	They have compared both theories with experimental data for surface currents gathered at Bugg Spring. [14]

10	Wilson (1988) [25] and Milgram and Erb (1984)	The value of the model constants used varies significantly. The cone angle is generally given as between 10-12°, although some sources quoted values of up to 23°. The lower values closely match that of 10° given by Wilson (1988) and Milgram and Erb (1984) [15]. However, it should be noted that this cone angle is defined as that of the subsea plume and does not include the effect of radial flow, which is known to occur near the sea surface.
11	Billeter and Fanne1op (1989)	Billeter (1989) and Fanne1op (1989) state that the 'boil area', where the bubbles break through the surface, has approximately twice the diameter of the bubble plume as determined in the absence of surface interaction. Although this observation is yet to be confirmed by detailed measurements, it would give an explanation for the use of cone angles of up to 23^0 [2]
12	Loes and Fannelop (1989) Billeter and Fannelop (1989)	They have undertaken measurements of the gas concentration above field scale and laboratory-scale underwater releases which show that the concentration profile appears to be Gaussian. The Integral model was used to compare predictions of bubble rise time for a variety of release rates against trials data (Loes and Fannelop (1989) using a range of established values for the entrainment coefficient (α), bubble terminal velocity, bubble drag coefficient etc. Reasonable agreement was achieved when the entrainment coefficient for the spherical cap was taken as 0.15. [12]
13	Moros and Dand (1990)	Described the application of the PHOENICS commercial CFD code to the calculation of surface current with an objective being to assess the displacement of vessels in the vicinity of the blow out. [20]

14	Fannelop, Hirschberg and Kuffer (1991)	Reported a comparison of theory and experiment for the case of a two dimensional surface current. [6]
15	Computational Fluid Dynamics (CFD) models by Moros and Ryall 1992	CFD involves the computation, on a suitable grid, of the solution to the Navier-Stokes equations of fluid motion. General purpose CFD models are now available and have been used in a range of applications, including dispersion of the above-sea part of a subsea release, (Moros and Ryall 1992). CFD modelling is resource-intensive, and requires careful setting up of boundary conditions and sub-models. It is particularly useful in determining the effects of obstructions, but is not in general use otherwise. [19]
16	Moros and Ryall (1992)	The distance to which the flammable envelope of the gas extends will depend on ambient conditions, such as wind speed and atmospheric stability, as well as the source conditions. The dispersion of the gas is typically modelled using Gaussian and integral models, for example the WS Atkins computer codes PLUME and SLUMP, which are used for buoyant gas and dense gas releases respectively. [19]
17	Swan and Moros (1993)	Extended the use of CFD to a comparison of such numerical predictions of bubble plume behavior with both experimental data and the results from integral models. [24]
18	Bettelini and Fannelop (1993)	Developed an integral model for the initial phase of subsea release due to a blow out or pipeline rupture. [1]
19	Navier-Stokes (1994)	Developed equation of fluid flow (CFD models)

20	WS Atkins Computer code (1997)	The assumption of similarity of plume concentration and velocity profiles is combined with entrainment relationships to produce a set of equations which are then integrated along the trajectory of the plume. Plume momentum and buoyancy, and ambient wind speed and turbulence all affect the dispersion through these modelled equations.
21	Hassan Abdulmouti and Tamer Mohamed Mansour (2006)	Particle Image Velocimetry (PIV) is used to measure the field flow velocity by analyzing the motion of the seeded particles in the flow. This data can be used for measuring the process parameter and this data can be used by CFD model for more accurate results. [10]
22	Fannelop and Bettellini (2007)	Developed plume model for very large bubble set in broken gas pipeline. [5]
23	Schalk Cloete et al (2009)	CFD modeling of plume and free surface behavior resulting from a sub-sea gas release. [23]
24	Hassan Abdulmouti (2011)	The gas flow rate, the bubble size and the internal two-phase flow structure of the bubble plume determines the characteristics of the surface flow. The structure of the bubble plume is studied in detail using numerical simulation (Eulerian-Lagrangian) model and by using flow visualization and image processing measurements. [9]

2.3 Review and analysis of existing plume discharge models

The following are the types of Subsea gas pipeline leaks discharge models commonly used in North Sea and Norwegian Sea.

   a. Empirical/ Cone model
   b. Integral Model
   c. Computational Fluid Dynamic (CFD) model

Empirical models are the simplest one which assume the plume radius to be proportional to the release depth or correlations that have been produced to fit the available experimental data.

The mathematical equations of hydrodynamics are the basis for the development of integral model and CFD.

In *Integral models*, the radial profiles of velocity and density are assumed to have a similar form at different heights within the plume. The plume properties can be represented, using for example Gaussian profiles, by their plume centreline values. A correlation relating to the rate of increase of water flow to the plume centreline properties through the use of an entrainment coefficient, as is used for including entrainment of water (liquid entrainment) in single phase plume modelling. Gas continuity, and equating the increase in momentum to the buoyancy forces, allows the plume properties to be calculated in a step-by-step manner as the height above the release is incremented. Separate models have been produced for the ZOEF and the ZOSF.

Computational Fluid Dynamics (CFD) is the most complex models which solve the Navier Stokes equations of fluid flow. Their advantage over integral models is that effects such as entrainment and turbulent transport of momentum are modelled directly and do not require the use of empirical constants. However CFD models still involve some modelling assumptions and are more resource-intensive to run than integral or empirical models as described below.

2.3.1 Cone/ empirical model

Taylor's study of line plumes used as breakwaters was initially published in 1955. Taylor Morton and Turner formulated the fundamental theory for turbulent single-phase plumes in 1956 [18]. Their paper has been a prime reference for later plume studies, first in

meteorology, and subsequently in bubble-plume hydrodynamics studies. Most relevant are the papers by Fanneløp and Sjøen (1980) [7] and the plume measurements published by Milgram (1983) [17]. A large number of studies, both in research and in engineering applications, are based on these papers.

Simple cone models assume either that the bubble plume has a cone of angle θ, or, equivalently, that the radius at the surface is a fixed proportion of the depth: i.e. b (z) =z tan (θ/2) his 'model' illustrated in Fig below.
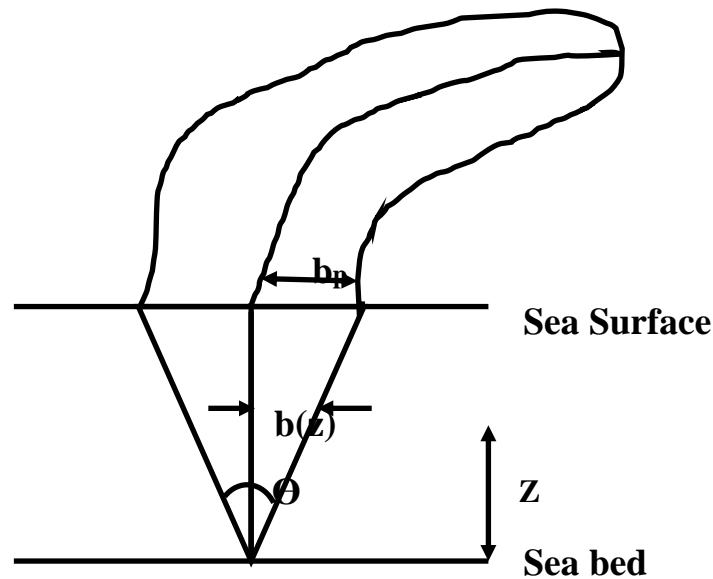
Fig: 2.1 Subsea discharge based on simple cone model

It is assumed that θ, and hence tan θ/2, are fixed parameters which do not vary with release rate or depth. The value of the model constants used varies significantly. Generally, the cone angle is given as between 10-12°. Lower values closely match that of 10° that is given by **Wilson, 1988** [25] **and Milgram and Erb, 1984** [15]. This cone angle is defined as that of the subsea plume and does not include the effect of radial flow, which is known to occur near the sea surface.

The 'boil area', where the bubbles break through the surface, has approximately twice the diameter of the bubble plume as determined in the absence of surface interaction. Although this observation is yet to be confirmed by detailed measurements, it would give a justification for the use of cone angles of up to 23^0 **Billeter and Fanne1op 1989** [2].

Uncertainty in Results from Empirical Model [22]:

These models are clearly the simplest of those considered, and has the following limitations:

a. They assume complete plume similarity through both the depth of the sea, and over the range of release rates considered;

b. There is no dependence of the diameter of the surfacing plume on the release rate;

c. No predictions are provided for concentration or gas velocity immediately above the surface;

d. Some uncertainty exists in the effective diameter at the surface, resulting in a factor of around 2 on recommended cone angles.

In view of these limitations, accuracy is not expected to be high especially for high release rates. However for moderate release rates in moderate water depths, the included angles at the lower end of the range should give a reasonable estimate of surface 'boil' diameter.

2.3.2 Integral Models

The dispersion of the gas from the release point to the surface is considered in three zones.
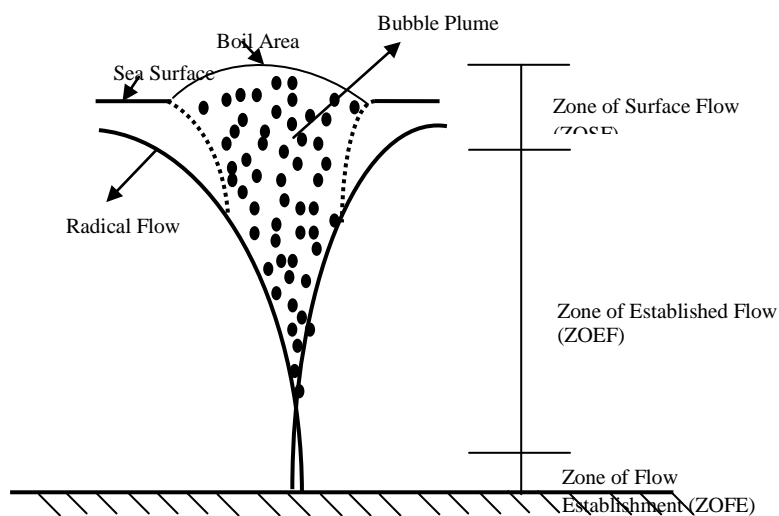
Fig: 2.2 Idealised subsea bubble plume

Zone of Flow Establishment (ZOFE): The region between the release point and the height at which the dispersion appears to adopt a plume-like structure. At this height the effects of initial release momentum are considered to be secondary to the momentum induced by buoyancy.

Zone of Established Flow (ZOEF): The plume-like region of dispersion which extends from the ZOFE to a depth beneath the free surface which is of the order of one plume diameter.

Zone of Surface Flow (ZOSF): The region above the ZOEF where the plume interacts with the surface causing widening of the bubble plume and radial flow of water at the surface.

2.3.2.1 Governing Equations (Integral Form)

The distance from the source is denoted by 'z' and the horizontal distance from the plume axis by 'r'. An over bar is used for all quantities dependent on both r and z, while this is omitted for quantities dependent only on z. The index (o) is used for values at the source. For quantities in the plume the index (p) is used, while the gas and water phases are denoted with the indices (g) and (w) respectively.
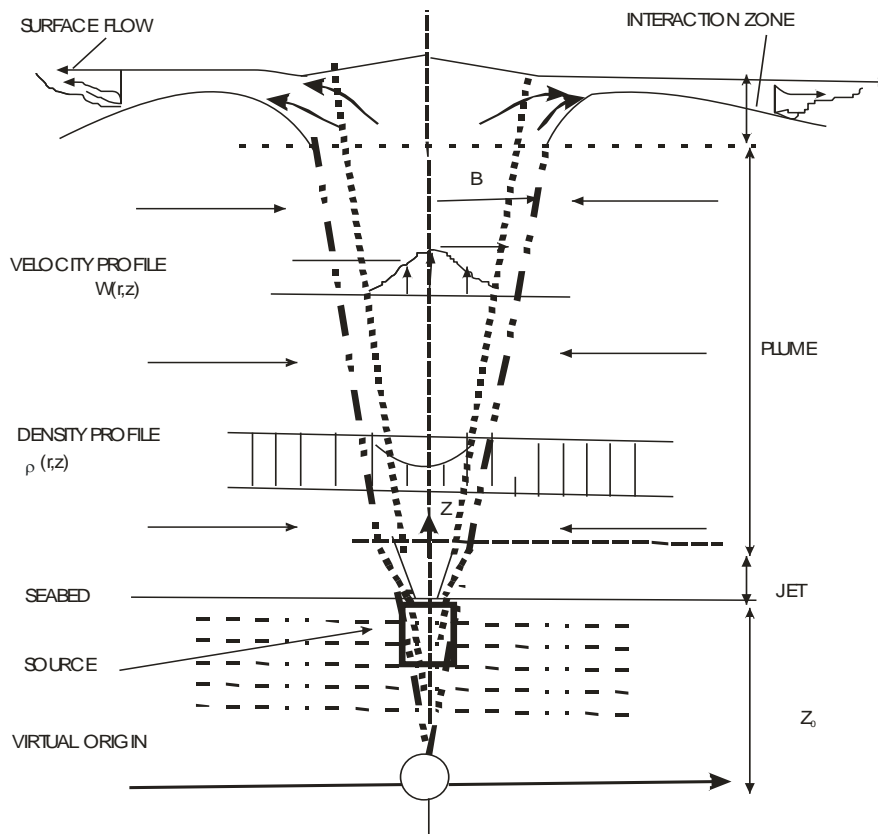
Fig: 2.3 Steady-state bubble plumes with surface flow

The gas expansion is represented by means of the polytrophic relation

$$\frac{\rho_g(z)}{\rho_g(0)} = \left[\frac{p(z)}{p(0)}\right]^{1/n} \qquad (eqn.-1)$$

The momentum equation for the plume established by Fannelop et al (2007) [5]

$$\frac{d}{dz}\left(\varphi_2 w^2 b^2\right) = \varphi_4 \frac{g\dot{V}_0}{\pi(w + \varphi_4 w_s)}\left[\frac{H}{H - z}\right]^{1/n} \qquad \textit{(eqn.-2)}$$

Empirical Coefficients

The empirical parameters required are summarized; estimates for the expected range of variation and the values recommended are presented in Table 6.1. The plume development is sensitive to variations in the entrainment coefficient α. Variations of the remaining parameters in their expected uncertainty ranges have only a minor influence on the results. Only results based on the Gaussian profile assumption is more realistic.

Gas expansion

The gas expansion is assumed to be isothermal (n = 1), as an adiabatic process would result in an unrealistically large drop in temperature for the rising gas.

Entrainment coefficient α

The entrainment coefficient α has had been found to increase with increasing gas flow rates. This can be accounted for by means of a semi-empirical correlation proposed by Milgram [17]:

$$\alpha = K \frac{F_r}{A + F_r} \qquad \textit{(eqn.-3)}$$

Width Ratio λ

The range of variation in λ is smaller and the effect on the plume development is much less important. The lower values correspond also here to laboratory experiments, whereas for very large scales λ is expected to approach unity.

Bubble Slip Velocity U_b

The typical values of bubble slip velocity are 28-30 cm/s for bubbles of 0.2-1.5 cm diameter. For larger diameters the value rises to 35-40 cm/s, but in the turbulent plume the bubbles tend to be unstable and to break up into smaller sizes. Milgram's [17] analysis is based on a value of 0.35 m/s. A slightly smaller value of 0.3 m/s will be used herein. Because the influence of this parameter is known to be weak, its effect will not be investigated in more detail.

Momentum Amplification Factor ϒ

The momentum amplification factor is defined as the ratio of total momentum flux to the momentum flux carried by the mean flow [17] and is a measure for the momentum flux due

to turbulent fluctuations. Large values of this parameter are found in small-scale laboratory experiments. This is the case also for the phenomenon known as plume wandering. As the bubbles become very small in comparison with the plume dimensions, bubble dynamics and interactions become less important and the flow behaves like a single-phase fluid. It follows that Momentum Amplification Factor can be expected to approach unity. This is confirmed by the analysis carried out by Milgram [17].

$$\Upsilon = \frac{M(z)}{2\pi \int (U2\ (U2(r,z)\ p\ f1 - f\ (r,z) + (U(r,z) + UJ\ 2p(z)f(r,z)r.dr.}$$

(*eqn.-4*)

Table 2.2 Recommended Values for empirical parameters for application:

S.No	Parameter	Range	Recommended Value
1.	n	1- c_p/c_v	1
2.	α	0.06 - 0.15	0.1
3.	λ	0.6 - 1.0	0.8
4.	U_b	0.1 - 0.4m/s	0.3m/s
5.	Υ	1-2	1

As shown by Fanneløp and Sjøen [7], the governing equations for a steady plume, Eqn. 1 and Eqn.2 admit a closed form similarity solution only if the slip velocity U_b is neglected and the buoyancy term in Eqn. 2 are constant. For distances from the source of the order of $p_a/ (g\ r_w)$, this is a reasonable approximation. The similarity solution is

$$b = \frac{6}{5}\frac{\alpha}{\varphi_1}z$$

(*eqn.-5*)

$$w = \frac{1}{2}\left[\frac{25}{6\pi}\frac{\varphi_1^2\varphi_4}{\varphi_2}\frac{g\dot{V}_0}{\alpha^2}\right]^{1/3}z^{-1/3}$$

(*eqn.-6*)

$$c = \frac{\varphi_4\dot{V}_0}{\varphi_3\pi b^2 w} = const.z^{-5/3}$$

(*eqn.-7*)

2.3.2.2 Integral models for the Zone of Established Flow (ZOEF)

The integral models are developed form physical processes model. The leading assumptions for bubble and plume dynamics have supported the development of integral models in a manner similar to that used for thermally buoyant plumes. The general integral formulation given by **Milgram, 1980** following on from a report by **Fazal and Milgram** [8], serves as a good example as described below.

Firstly, the mean fluid velocity, and the mean density defect within the plume are assumed to take the form of Gaussian distributions, i.e.

$$U(r,z) = U(z)\, e^{\frac{r^2}{b^2}} \qquad\qquad (eqn.\text{-}8)$$

$$\rho_w - \rho_p\,(r,z) = S(z)\, e^{\lambda^2 \frac{r^2}{b^2}} \qquad\qquad (eqn.\text{-}9)$$

Rew et al [22] have solved the following equations using a numerical integration scheme which approximates derivatives in z using a simple finite difference, scheme, and then solves for the centreline gas fraction $S(z)$, the centreline velocity $U(z)$ and the plume width $b(z)$ using Newton iteration.

$$2\alpha U(z).b(z) = \frac{d}{dz}\left[U(z).b^2(z) \quad 1 - \frac{\lambda^2 S(z)}{[1+\lambda^2][\rho_w + \rho_g(Z)]} \right] \qquad (eqn.\text{-}10)$$

$$\left\{ \frac{q_T H_T}{H_B - z} = \frac{\pi\lambda^2 b^2(z)S(z)}{\rho_w - \rho_g(z)}\left[\frac{U(z)}{1+\lambda^2} + U_b \right] \right\} \qquad (eqn.\text{-}11)$$

$$g\lambda^2 S(z)b^2(z) = \frac{d}{dz}\left[\gamma b^2(z)\left\{ U^2(z)\left[\frac{\rho_w}{2} - \frac{\lambda^2 S(z)}{1+2\lambda^2} \right] + \frac{\lambda^2 U_b \rho_g(z)S(z)}{\rho_w - \rho(z)}\left[\frac{2U(z)}{1+\lambda^2} + U_b \right] \right\} \right] \qquad (eqn.\text{-}12)$$

2.3.2.3 Integral models for the Zone of Surface Flow (ZOSF)

The mass flux integral equation for Integral models for the Zone of Surface Flow is written as:

$$m_F = \rho_w 2\pi r \int_0^\infty V(r,Z)dZ$$

(eqn.-13)

and the momentum flux of the fluid as:

$$M_P = \rho_W 2\pi r \int_0^\infty V^2(r,Z)dZ$$

(eqn.-14)

As with the vertical plumes, conservation laws for mass and momentum are applied in the form of an entrainment relation for the former, and the assumption that no external forces (i.e. buoyancy or viscous effects) are acting on the radial flow, giving:

$$\frac{d}{dr}\left(\pi^{\frac{3}{2}} \rho_w h_w V_w r \right) = 2\pi r \rho_w \beta V_m \ and$$

(eqn.-15)

$$\frac{d}{dr}\left[\left[\frac{\pi^3}{2}\right]^{\frac{1}{2}} \rho_w h_w V_w^2 r \right] = 0$$

(eqn.-16)

Uncertainty in results from Integral Models [22]:

The accuracy of the integral models is most sensitive to:

a. the need for an established zone of plume-like behaviour;
b. the entrainment assumption, and the constancy of coefficients and for the plume and the free surface flow region;
c. the treatment of the bubble plume as a continuum, based upon the assumptions regarding bubble dynamics cited in section Bubble Dynamics;
d. the value of λ deduced from experimental observation.

However it is not clear how closely full scale blowouts conform to the plume-like model which forms the basis of the integral formulation, since the gas flow rates used in experiments are so low. It might even be the case that the so called zone of flow

establishment is the dominant region for gas flow rates of 30Nm^3/sec or more in 'shallow' water depths of 30-40m, typical of the southern part of the North Sea and Norwegian Sea.

The experimental data point towards the entrainment assumption being inappropriate even for small scale experiments. The evidence for this conclusion relates to the apparent dependence of a continuous gas flow rate, bubble plume radius, centreline velocity, turbulence intensity and bubble separation as cited by **Fannelop and Sjoen 1980** [7].

2.3.3 Computational Fluid Dynamics (CFD) Models

Three different multiphase CFD methods were evaluated to assess their applicability by Schalk Cloete et al [23]. These include the Eulerian-Eulerian multi-fluid approach, the Eulerian-Eulerian mixture model and also a combined model consisting of the Eulerian-Lagrangian discrete phase model (DPM) and the Eulerian-Eulerian volume of fluid (VOF) model. The VOF variant of the Eulerian-Eulerian multiphase approach is specifically designed for the tracking of sharp interfaces between various phases and the bubble plume was tracked with the DPM. The coupled DPM and VOF model was therefore identified for quantitative studies of subsea gas release. The VOF model solves for conservation of mass as represented by below equation.

$$\frac{d}{dr}(r_\phi \rho_\phi) + \nabla.(r_\phi \rho_\phi U_\phi) = m \qquad (eqn.\text{-}17)$$

$$\frac{d}{dt}(r_\phi \rho_\phi U_\phi) + \nabla.(r_\phi \rho_\phi U_\phi.U_0 - r_\phi T_{F\phi} \nabla U_\phi) = r_\phi S_{F\phi} \qquad (eqn.\text{-}18)$$
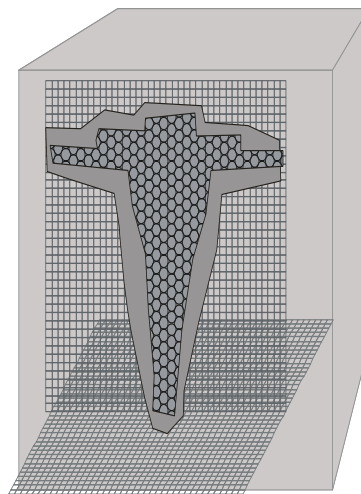
Fig 2.4 Cross section of the grid used in the coupled DPM-VOF simulation

The DPM tracks discrete particles through the domain in the Lagrangian sense by implementing a force balance over each particle:

$$\frac{d\vec{u}_p}{dt} = F_D\left(\vec{u} - \vec{u}_p\right) + \frac{\vec{g}\left(\rho_p - \rho\right)}{\rho_p} + \vec{F}_p \qquad (eqn.\text{-}19)$$

The bubble trajectory is predicted by integrating the equation of motion (Domgin et al):

$$\frac{dv}{dt} = F_D(u - v) + g(\rho_p - \rho)\Big/ \rho_p + \frac{1}{2}\frac{\rho}{\rho_p}\frac{d}{dt}(u - v) + \frac{\rho}{\rho_p}\frac{du}{dt} \qquad (eqn.\text{-}20)$$

A Lagrangian equation of motion for each discrete bubble was given as:

$$\rho_g(z)\frac{dV_i}{dt} = -\frac{3\mu_i}{4d_b}(V_i - U_i)C_D R_e + \rho_w U i\frac{\partial U_i}{\partial x_i} - \frac{\rho_w}{2}\left[\frac{dV_i}{dt} - U_i\frac{\partial U_i}{\partial x_i}\right] - (\rho_w - \rho_g(z))g_i$$

$$(eqn.\text{-}21)$$

Equation 21 represents a balance between the bubble acceleration, bubble drag, pressure gradients, bubble added inertia forces and buoyancy.

The generation of turbulence by the bubbles is modelled by assuming that production and dissipation are in balance, and that therefore the total turbulent kinetic energy generated within each cell is;

$$P_b = \frac{q(z)}{N\Delta V}\sum_{n=1}^{N} F_i(V_i - U_i)dt \qquad (eqn.\text{-}22)$$

Thus the turbulence production is due entirely to the sum over all bubbles in a cell of the power ($F_i(V_i - U_i)$)) required to overcome bubble drag, integrated over the time taken by the bubble to traverse the cell.

Uncertainty in Results from CFD Models [22]:

The main sources of uncertainty for CFD models concern:
   a. the implementation of additional source terms in conventional CFD codes;
   b. the need for very specific and detailed flow data for validation purposes.

The additional source terms required in the momentum and turbulence transport equations are based upon many of the assumptions on bubble dynamics described earlier. It is not clear

how well these behave when the volume fraction of liquid is low, as would be the case for high gas flow rates.

Secondly, the problem of validating CFD models in general is exacerbated by the need for detailed measurements of velocity distribution, turbulence etc. It is difficult to measure such quantities accurately for two phase flows.

2.4 Critique of existing literature

The majority of experimental programmes have been carried out at laboratory scale. Of the two sites used for field trials by Topham (1975) at Saarich Inlet, Vancouver Island and Milgram et al (1983,1984) at Bugg Spring neither were able to carry out tests at realistic gas flow rates, although the water depths used were appropriate to shallow coastal waters.

The small scale experiment of Kobus (1968) is the first of its kind. Point source bubble plumes at both sonic and subsonic gas release velocities were used and a Gaussian curve fitted to velocity profiles. There was some evidence of unsteadiness in the results arising from plume wandering. This data was later used by Ditmars and Cederwell (1974) both to calibrate and validate their integral model of bubble plume hydrodynamics.

Full scale trials of Topham were carried out at 23m and 60m water depth, and with air flow rates of up to $0.66Nm^3$/s and $O.45Nm^3$/s respectively. Whilst these flow rates are low by comparison with likely values from a full pipe rupture, they represent (along with the experiment of Milgram) the upper values of flow rates used in experimental work. The principal observation in this work related to the variation in centreline velocity and plume width with depth, being initially conical, in line with entrainment models, but then remaining constant for some portion of the depth before further expansion near the surface. This was not observed to be the case for releases at 23m, in which the conical form of the plume was retained throughout.

A well defined wave-ring was observed in these experiments, and an expression for its radius derived by data fit to be:

$$R = 0.39\, z\left\{ \frac{10.36 V_8}{Z + 10.36} \right\}$$

where

z   =   water depth (m)

V_8 =   Volume flow rate of gas at surface (m^3/s)

Milgram comments that the Topham data contains considerable evidence of unsteadiness, due in part to the lack of lateral restraint of the apparatus upon which the current meters were mounted, and some evidence of plume wandering.

The experiments carried out by Mc Dougall (1975) were notable in that an attempt was made to examine the effect of density stratification. Again the flow rates and water depth were at very small scale. The mechanism of most interest in this case, namely the 'removal' of a portion of the entrained liquid at the density interface was observed. However, it was not possible to compare the mathematical model developed for the double plume structure with experiment, since some of the modelling assumptions were invalid for the experimental scale, and it was thought that the measured data would be affected by the restricted size of the tank used.

Fazal and Milgram (1980) reported experimental data, again at small scale, in which the assumption of a conical plume structure driven by entrainment appears valid. They comment that this is the case for the time averaged data but that the plume appears to be very unsteady, particularly in the horizontal phase.

The experimental work of Fannelop and Sjoen (1980) was again carried out at laboratory scale. The stated purpose of the experiments was to establish more detailed information on plume structure, both in the Zone of Established Flow (ZOEF) and at the free surface. In particular they sought to reduce uncertainties regarding the value of λ, the ratio of the bubble region width to the total plume width. As before, plume unsteadiness was cited as a cause of uncertainty in the results obtained, as were a number of issues regarding the appropriateness of the instrumentation for measuring the velocity of a two phase flow. Their results indicated

that a Gaussian data fit to the velocity profile was good to a confidence level of 90% for all flow rates tested. The subsea entrainment coefficient (α) showed some dependence on flow rate but was of similar magnitude to that measured by others. Surface flow velocities were also measured, and a surface entrainment coefficient (α) of approximately 0.06 appeared appropriate.

Milgram and Van Houten (1982) also reported comparisons of computations with experimental data for both the Zone of Established Flow (ZOEF) and some portion of the free surface region. Again this was at small water depths and low flow rates, for which the Gaussian plume integral models appeared to give reasonable predictions. They were also able to establish by experiment that approximately 50% of the momentum flux was transported by turbulence, leading to an improvement in their modelling predictions at this scale. For the Zone of Surface Flow (ZOSF), comparisons of predictions of velocity distributions with measurements by Fannelop and Sjoen (1980) revealed quite large errors.

Much of the preceding experimental work was reviewed by Milgran (1983), who went on to present a range of comparisons of computed results with field trials (Bugg Spring) data, and small scale data from Fannelop and Sjoen (1980) and Milgram and Van Houten (1982). These experiments and computations appear to confirm that:
   a. the ratio λ tends to 1.0 for full scale;
   b. the subsea entrainment coefficient a is a function of gas fraction, but is also dependent upon plume radius, bubble vertical speed, and bubble spacing;
   c. the small scale used in experiments leads to higher values of momentum flux generated by turbulence than would be the case at full scale;
   d. plume wandering found in previous experiments may be partially due to interaction with the tank walls.

Further work on the behaviour of the free surface flow region was reported by Milgram and Burgess (1984). Experiments carried out at Bugg Spring measured the velocity of the radial free surface flow using a simple float. The experimentally measured velocity profiles were

compared with computations, with good comparisons achieved by optimising the choice of entrainment coefficient for each gas flow rate.

Work on the structure of the free-surface flow and zones of re-circulation was also reported by Fannelop, Hirschberg and Kuffer (1991), wherein experiments carried out in a towing tank with a line source of bubbles was reported. On this occasion the surface entrainment coefficient β was found to be less dependent upon g flow rate, with computations using an integral model providing a poor fit to measure data.

Finally, Swan and Moros (1993) have provided a fairly thorough small scale comparison of experimental results with both integral and CFD models of bubble plumes. Again the experimental data for density defect and fluid velocities appeared well fitted by a Gaussian distribution. Radial flow velocities at the surface were also measured. The principal conclusion from this work was that, at least at this scale, the CFD computations provided superior predictions.

Taylor used an entrainment model in his formulation of the plume equations. The inflow into the plume from the exterior flow (at rest) is here assumed to be proportional to the characteristic plume velocity and to the plume circumference or "surface of contact". The velocity and density profile shapes are assumed to be known (Gaussian or "Tophat"), and the bubbles are assumed to occur inside a radius λ r where λ typically has the value 0.8. This value as well as the constant of proportionality α (= entrainment coefficient) is determined from experiments, typically α = 0.06 - 0.1. Prior to solving the plume equations of motion, they are integrated over the cross-section using the values and profiles suggested above. The integral method gives good results, i.e. the calculations are as accurate as the available measurements and often better. A particular problem associated with plume flows, is the swaying or lateral motion of the plume. To get repeatable results, the measurements will have to be averaged over time intervals of the order of minutes.

An alternative to this approach is to simulate the plume flow by means of a general purpose Navier-Stokes solver, such as PHOENICS. Many have tried this approach, among them Lindholm (1995). His method is an adaptation of simulation techniques that have been tried successfully in bubble columns. Bubble plume doesn't act like a "pump" lifting fluid towards the surface. The rising fluid has the shape of a slender pencil and not that of a rapidly

growing plume flow. The rising flow does not "entrain" fluid from the exterior water mass and there is too little inflow into what should be the plume. The problem appears to be related to the "distant" boundary condition used in the simulation. In the bubble column the lateral inflow is zero, due to the sidewall. This is not the case for the unconfined plume. The integral formulation used by Taylor produces both the "correct" inflow locally into the plume and also at large distance away from it. The correctness of his approach follows from fundamental hydrodynamics.

2.5 Chapter Summary

The understanding about the behaviour of a subsea gas release up through the water column is limited from safety sensitivity study point of view. The hydrodynamic basis for bubble-plume flows is reasonably well understood, but the solutions of the associated equations, depend on a large number of parameters that can only be evaluated from experiments.

Numbers of lab scale experimentations were conducted in UK and Norway for modelling the discharge of subsea releases. Three approaches of varying complexity have been used.

a. Empirical/ Cone model
b. Integral Model
c. Computational Fluid Dynamic (CFD) model

An important consideration when using subsea dispersion models is the resource required to use them, potentially for a large number of scenarios. *Clearly, the simple empirical model is the least resource-intensive, user-friendly and, reasonably accurate, and hence the most favoured for use in safety sensitive studies and risk assessments.*

Table 2.3 Comparison of Models

S.N	Types of models	Accuracy	Uncertainty	Cost	User-friendliness
1	*Empirical*	Medium	Medium	Low	High
2	*Integral*	Medium	Medium	Medium	Medium
3	*CFD*	High	Medium	High	Low

3. RESEARCH PROBLEM

3.1 Chapter overview

This chapter introduces the research problem, highlights the implications of the research problem and the influence of research problem on off-shore Exploration and Production (E&P) companies operating in Arabian Sea.

3.2 Introduction to Research Problem

The field of consequence modelling for hydrocarbon releases in open atmospheric conditions is highly developed and has evolved over a period of time in stages as explained below:

Table 3.1 Stages of Development of Atmospheric dispersion models

Stages	Year	Developments/ Advancements in the field of Atmospheric gas dispersion models
Stage-1	Early 80's	No computer software was available to predict the consequences of hydrocarbon releases. Only equations from the books were used to calculate the consequences.
	1985	WAZAN, software was developed by M/s Technica sponsored by UN. This software had stand alone modules for basic consequence analysis. The equations were taken from available academic literature e.g. Gaussian dispersion equation used for gas dispersion modelling.
Stage-2	1990s	HD Gas model was developed as Gaussian plume model proved not to be correct for heavier than air gases.
Stage-3	Late 1990s	Standalone models were transformed into toolkits where transition from one module to another can be automatic rather than based upon analyst judgment.
	2000+	A lot of experimental works were carried out in the field of Hydrocarbon release consequences analysis and the case histories damage information available has been used to fine-tune the models.

The dispersion of the gas is typically modelled using Gaussian and integral models, for example the WS Atkins computer codes PLUME and SLUMP, which are used for buoyant gas and dense gas releases respectively. [19]

As of today only limited research work is done to study and model subsea gas pipe line leaks discharges. In UK, Health and Safety Executive (HSE), Det Norske Veritas (DNV) and Shell Global Solutions have done some research in this area. Similar studies were carried out by Petroleum Safety Authority (PSA), Norway for lower sea depths ranging 100-400 m.

So far no such research work is done in Arabian Sea for higher depths ranging 500 to 1500 m.

3.3 Implications of research problem

The effects of a subsea release as the hydrocarbon plume reaches the surface will depend on a number of factors, including whether the release is liquid or gas. For a liquid release, the buoyancy will result in the leaked material spreading on the surface to form either a polluting slick, or an expanding pool fire. For a gas release, although the buoyancy is rather greater, significant drag forces will cause the plume to break up and rise to the surface as a series of bubbles.

    a. On breaking surface, ignition of the gas plume would result in a sea surface fire with different characteristics to those incorporated into the usual pool and jet fire models.

    b. Alternatively, and more likely, the plume will begin to disperse in the atmosphere, and may be diluted to a concentration below the lower flammable limit before there is any possibility of encountering an ignition source.

    c. A further effect of a gas bubble plume is the reduction in the stability of floating vessels, due to either the loss of buoyancy, or, more likely, due to the radial outflow of water which has been entrained into the plume.

The better the understanding of subsea gas pipeline leak scenarios for a specific sea conditions, the accuracy of safety sensitive studies & consequence analysis shall be greatly improved and specific controls can be put in place to manage the resultant safety risks.
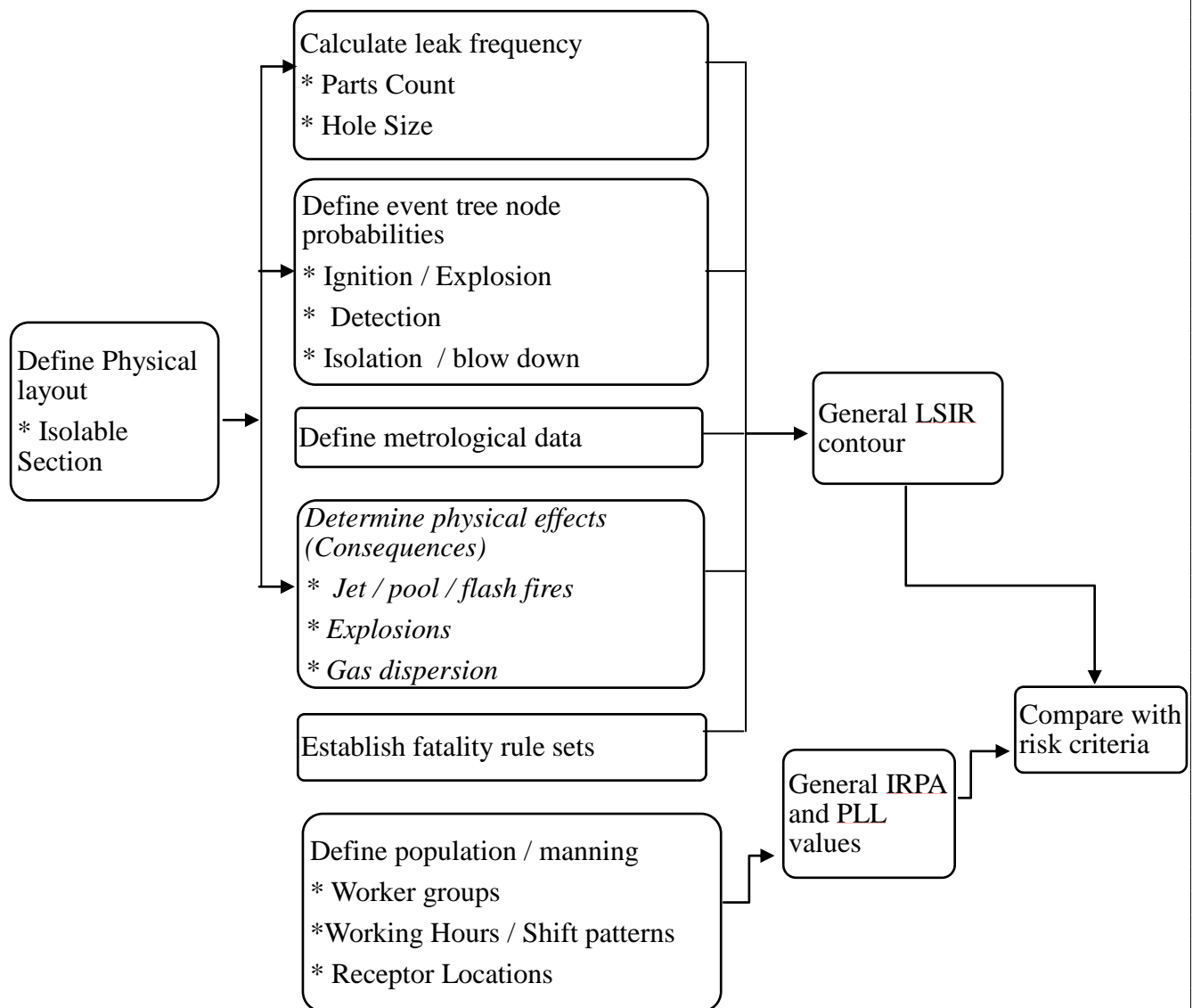
Fig: 3.1 Risk Assessment Framework

3.4 Influence of research problem on Off-shore Oil and Gas industry

The outcome of this research will help in assuring the accuracy of safety sensitive studies and consequence analysis of the sub-sea gas pipelines leaks for higher Sea depth scenarios ranging 500 m to 1500 m.

3.5 Chapter Summary

Consequence models are used to predict the physical behaviour of hazardous incidents mainly flammable and toxic releases. Some models only calculate the effect of a limited number of physical processes, like discharge or radiation effects. More complex models interlink the various steps in consequence modelling into one package.

The field of consequence modelling for hydrocarbon releases in open atmospheric conditions is highly developed, and there are several commercially available computer programs to model the discharge, dispersion and fire/explosion effects of gases and liquids. Some of these techniques are relatively simple, and are suitable for manual analysis, and have commonly been implemented in customized spread sheets. More complex models are available in stand-alone format and also as part of linked software or toolkits.

Whereas as of today only limited research is done in UK and Norway to establish the sub-sea gas pipelines leaks discharge models for sea depths ranging 100 m - 400 m. No such research is done for higher depths ranging 500 to 2000 m i.e. for Arabian Sea Conditions.

As the on-shore Oil & Gas resources are fast depleting, the need for deep sea Oil & Gas Exploration and Production (E&P) is inevitable in near future. Due to this requirement, several kilometres of sub-sea oil and gas pipelines need to be laid. Going by the past case histories, the sub-sea gas pipelines are more vulnerable for failures due to corrosion and mechanical damages. Such failures may lead to major safety incidents. In this context, studying and modelling of deep seated Gas Plume discharge scenarios is gaining importance from safety point of view.

4. RESEARCH METHODOLOGY

4.1 Chapter overview

This chapter outlines the objectives of this research, methods and materials involved. It outlines the sub-sea gas bubble plume calculation basis, usage of past experimentation results, uncertainty of past experimentation, scale refinement, algorithms used for IIT experimentation, and the limitations.

4.2 Objectives

The objectives of this thesis are:

a. To identify various sub-sea gas discharge models that are currently being used in North Sea and Norwegian Sea with respect to plume discharge (initial release of plume to the sea surface from the point of leak);

b. To study and analyse the accuracy and uncertainty levels of various discharge models used in North Sea and Norwegian Sea based on the feedback received from lab scale experimentation and limited filed trials carried out so far;

c. Identify the most optimal discharge model suitable for Arabian Sea conditions striking a right balance between i) accuracy, ii) uncertainty, iii) cost-effectiveness and iv) user-friendliness;

d. Validate the chosen model for Arabian Sea Conditions based on lab-scale experimentation and CFD Modelling.

4.3 Materials & Methods

4.3.1 Numerical modelling Vs. Analytical modelling

Numerical modelling is all about quantitative prediction of the behaviour of a physical system through numerical operations, whereas Analytical modelling is based on experimentation and facts. The result of analytical modelling/ analysis is often a functional relation given in a formula or graph, which covers a range of dependent and independent variables often in combinations in non-dimensional numbers. In contrast, the numerical model gives the specific solution in terms of numbers based on initial and boundary

conditions. From Scientific point of view, numerical models are mostly preferred. But the engineering perspective is to use not only the best but also the most reliable and accepted principle to the actual situation and hence importance of analytical modelling can't be ignored.

One problem associated with designing suitable experiments is that of scaling. For air bubbles rising in a plume in a water tank, the "typical" bubble size will be about 10 mm regardless of whether the tank is 1 m or 10 m deep. This means that the bubble dimension relative to our plume (or flow) dimension will not be the same. The bubble size will be largely determined by the surface tension gas-to-water, and it is difficult to tailor this to fit desired scaling relationships. (The presence of hydrocarbons in the gas will reduce the surface tension and hence the bubble size, but not enough to make much difference. For reasons of safety, most laboratory experiments are carried out using air. For offshore tests, natural gas may be a practical alternative.)

In the laboratory 02-05 m appears to be a practical upper limit for the plume depth whereas in offshore applications 50 m to 500 m could be of interest. In recent years a number of laboratory experiments have been reported with tank depths of the order of 1 m. Many recent studies appear to be directed towards metallurgical problems. This study is focused on safety problem.

4.3.2 Subsea gas bubble plume calculation basis

The gas bubble plume calculations are based on the following input data:
   a. Discharge depth H_0, m
   b. Gas mass flux q, kg s^{-1} m^{-2}
   c. Gas density r, kg/Sm^3 (@ 1 atm and 15^{0}C)
   d. Sea temperature Θ_s, ^{0}C

Here, the gas mass flux is presumed to be delivered by the subsea gas leak module in terms of a table of leak rates and corresponding times from the start of the leak. The gas mass flux is used together with discharge depth, sea temperature, and gas density to determine the volume flow rate V_0 (m^3/s) at the discharge depth:

$V_0 = q / \rho_0$

Where $\rho_0 = \rho \dfrac{H_0 + 10}{10} \dfrac{273 + 15}{273 + \theta_s}$ assuming ideal gas

In the expression above, the number 10 corresponds to 10 m water column, which equals a hydrostatic pressure of one atmosphere. The volume flux at the discharge depth is used to define the buoyancy flux parameter

$\phi_0 = gV_0 / \pi$

The bubble plume calculations are based on Fanneløp's general non-dimensional solution for Underwater gas releases, shown in graphical form at Figure B.1 (Fanneløp and Sjøen 1980, Fanneløp 1994). The critical assumption in the development of the solution is that the mass flux of gas is conserved, while the gas volume varies with hydrostatic pressure according to the ideal gas law. The expansion of the gas is assumed to be isothermal. Moreover, the initial momentum of the discharged gas is neglected, as well as possible effects of cross flow and stratification (due to vertical temperature and salinity gradients). This implies that the solution is valid for large gas leaks at moderate depths, but may be less reliable for small leak rates and large water depths due to enhanced influence of factors such as cross flow, stratification and dissolution of gas in the water masses (Johansen 2000).

The plume is defined by three variables – plume radius *bp*, centerline velocity *wp*, and plume rise time *tp* – all functions of the vertical distance *z* from the discharge point. These variables may be expressed in terms of non-dimensional variables, *X*, *B*, *W* and *T*:

X=z/H, B=b_p/2αH, W=w_p/M and T=t_pM/H

Where

$H = H_0 + 10$

$M = \left[\phi_0 \dfrac{\lambda^2 + 1}{2\alpha^2 H} \right]^{1/3}$

$\phi_0 = gV_0/\pi$

Fanneløp's non-dimensional general bubble plume model

Plume variables, all given as a function of the distance z (m) above the leak point:

bp: plume radius, m

wp: plume velocity, m/s

tp: rise time, s

The non-dimensional plume rise time T is derived from the non-dimensional plume velocity by the integral

$$T = \int_0^x dX / W$$

The parameter α is the entrainment coefficient ($\alpha = 0.1$), and λ is a shape factor representing the ratio between the buoyancy and velocity profiles ($\lambda = 0.65$), both assumed constant with depth.

4.3.3 Experimentation basis

The hydrodynamic basis for bubble-plume flows is reasonably well understood, but the solutions of the associated equations, depend on a large number of parameters that can only be evaluated by experimentation.

Experiments were conducted to observe real time gas plume behaviour underwater for the given conditions. Lab-scale experiments were carried-out for various flow rates and depths. The physical data obtained from experimentation were used to validate the theoretical models.

4.3.4 Usage of Past experimentation results

Based on the quality of data and documented results, following past experimental data were considered for evaluating the present study.

Tab 4.1: Past experimentation results

S.N	Authors	Water depth	Flow rate
1	Fannelop T.K., Sjoen K (1980)	10 m	0.005 - 0221 Nm^3/s
2	Milgram (1983)	50 m	0.024 - 0.590 Nm^3/s
3	Engebretsen et al. (1997)	7 m	0.083 – 0.75 Nm^3/s

4.3.5 Uncertainty of past experiments

The principal sources of uncertainty in the data provided by past experiments and field trials are:

a. the difficulties experienced in measuring fluid phase velocities within a two phase flow using conventional flow meters or laser Doppler anemometry;

b. the difficulty in determining the position of each instrument accurately within the bubble plume;

c. the observation that experimental rigs are themselves subject to movement within the flow;

d. the need to take long time averages of the data, but with little knowledge of the dominant time and length scales of the flow;

e. The use of very low gas flow rates in laboratory scale tests, and flow rates in field trials some two orders of magnitude smaller than that likely for a full scale blow-out;

f. The limited depth of water available in lab-scale tests.

The first three points may be overcome by suitable future design of experiments. The need for more measurements in water depths of 50m and above is also felt necessary. However, the main uncertainty is the lack of any data relating to plume behaviour at realistic release rates. It is currently assumed that the zone of established flow (ZOEF) begins in close proximity to the release source. For high release rates, a substantial part of the subsea plume may actually remain in the zone of flow establishment (ZOFE).

4.3.6 Scale refinement

In the laboratory 10 m appears to be a practical upper limit for the plume depth whereas in offshore applications 50 m to 500 m could be of interest. In recent years a number of laboratory experiments have been conducted with tank depths of the order of 1 m. Most laboratory experiments used gas flow rates of less than 1 kg/s [5]. Source diameter of 1" is chosen based on the real case data available for pipeline failures recorded by HSE Executive, UK.

A test tank of 1m depth and shallow water basin of 1.5 m was used for IIT experimentation with the scale: 1: 100.

4.3.7 Algorithms used for IIT Experimentation

a. Flow measurement

Gas flow was measured using Omega FL 46300 in line Flow meter.

b. Temperature measurement

Lab test basin sea water temperature was measured using thermometer

c. Salinity

Salinity data for Arabian Sea was obtained from NIOT website (www.niot.res.in)

d. Plume height and radius measurement

The video recording was done using the underwater camera Olympus 1050 SW 3m water proof. The radius of the plume and the height were measured in computer screen scale and then converted to actual scale.

e. Velocity Calculations

Velocity= Distance/Time

Time interval Δt is measured between one video snap shot to another.

For e.g. Distance measured is=50 cm (0.5m)

Time interval Δt =0.1s

Velocity=0.5m/0.1s=5m/s

Similarly all the readings for Velocity were calculated for the distances from 0.5m to 1.5m

Time interval Δt varies from 0.06s to 0.45s

For all the readings the graphs are shown.

Centreline velocity for various depths and gas flow rates were calculated as follows:

Centreline Velocity (V) = Distance from the source (H_0) /Time (Δt)

H_0 was measured using a graduated scale fixed on the experimental basin.

Δt - is the difference of time recorded for the particular depth by using the under-water camera

Table 4.2: Plume velocity at different flow rates

S.N	Flow Rates (V_g)	Plume Velocity
A	For gas flow rate (V_g) = 0.00253	
1	V= 0.5/0.1	5 m/s
2	V= 0.75/0.17	4.4 m/s
3	V= 1/0.256	3.9 m/s
4	V= 1.5/0.416	3.6 m/s
B	For gas flow rate (V_g) = 0.00505	
1	V= 0.5/0.069	7.2 m/s
2	V= 0.75/0.134	5.6 m/s
3	V= 1/0.208	4.8 m/s
4	V= 1.5/0.416	4.4 m/s
C	For gas flow rate (V_g) = 0.00758	
1	V= 0.5/0.053	9.4 m/s
2	V= 0.75/0.096	7.8 m/s
3	V= 1/0.15	6.6 m/s
4	V= 1.5/0.283	5.3 m/s
D	For gas flow rate (V_g) = 0.0112	
1	V= 0.5/0.045	11.1 m/s
2	V= 0.75/0.076	9.9 m/s
3	V= 1/0.134	7.43 m/s
4	V= 1.5/0.245	6.12 m/s

4.3.8 Limitations

One problem associated with designing suitable experiments is that of scaling. For air bubbles rising in a plume in a water tank, the "typical" bubble size will be about 10 mm regardless of whether the tank is 1 m or 10 m deep. This means the bubble dimension relative to plume (or flow) dimension will not be the same. The bubble size will be largely determined by the surface tension gas-to-water, and it is difficult to tailor this to fit desired scaling relationships. The presence of hydrocarbons in the gas will reduce the surface tension and hence the bubble size, but not enough to make much difference. *For reasons of safety, most laboratory experiments are carried out using air.* For offshore tests, natural gas may be a practical alternative. Momentum loss due to downward and sideward release is not considered. The effect of sea current on plume radius is not taken into account.

5. Experimentation at IIT

5.1 Experimentation facility

Lab scale experimentation was held at Department of Ocean Engineering, Indian Institute of Technology (IIT), Madras for validating the Empirical/Cone gas discharge plume model established by T.K.Fannelop and M.Bettelini, 2007 [5] for North Sea and Norwegian Sea (i.e.100-400 m depth) for Arabian Sea conditions (i.e. for 500-1500 m depth).
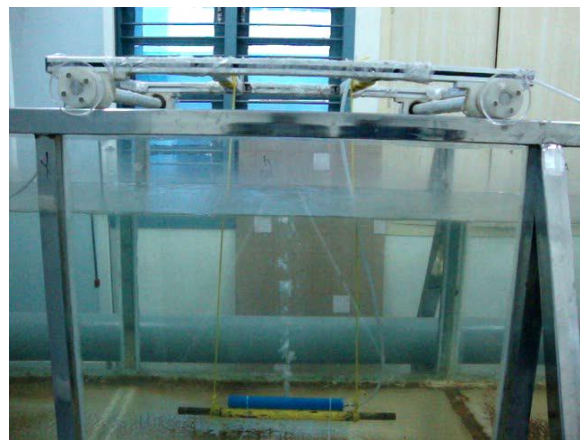
Fig 5.1: Wave basin facility at IIT. 30mx30mx3m deep equipped with Multi-Element Wave Maker (MEWM), 52 paddles capable of producing short and Long Crested Waves Maker (LCWM) capable of producing regular and random waves.

Fig 5.2: Test tank 2mx1.5mx1.25m height with graduation scales fitted for measuring plume height and diameter.

| Fig 5.3: Pespex pipe of 2inch diameter and12inches length with 1inch aperture with 3/4th inch brass gas inlet nozzle. | Fig 5.4: Pespex pipe assembly connected to 3/4th inch air hose with rope and mounting arrangement with dead weight. |

| Fig 5.5: Vertical graduation scale attached to test tank | Fig 5.6: Horizontal graduation scale attached to test tank |
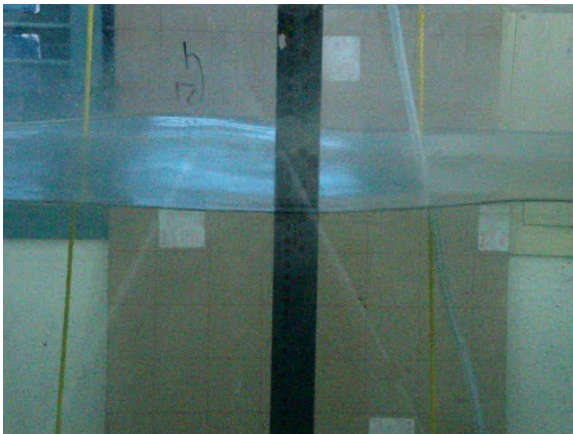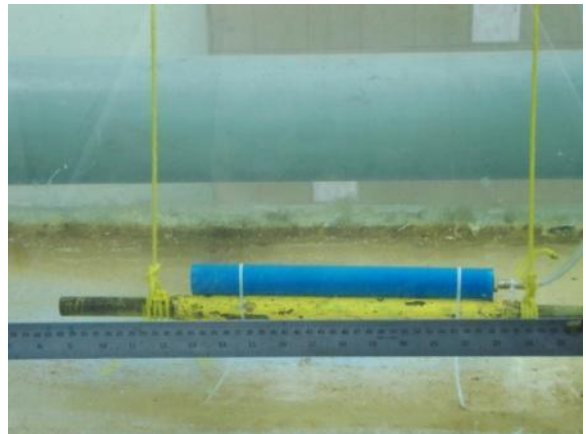
5.2 Experimentation Parameters

Table 5.1: Parameters considered for Experimentation

S.N	Parameters	Used in T.K.Fannelop and M.Bettelini experimentation	Used in IIT experimentation
1	Flow media	Air due to safety reasons.	Air
2	Height of water column (Sea depth)	50 m 100 m 200 m 300 m 400 m Scale 1:100	500 m 750 m 1000 m 1500m Scale 1:100
3	Leakage/ Flow rates	$0.00253m^3/s$ $0.00505m^3/s$ $0.00758m^3/s$ $0.0112m^3/s$ In the Risk Level Project, hydrocarbon leaks are categorized into three groups according to the leakage rate: • Major leak Greater than 10 kg/s (kg per second), • Medium leak 1 – 10 kg/s and • Minor leak 0.1-1 kg/s. [11] Even a gas leak with the lowest recorded leakage rate (0.1 kg/s) has a considerable accident potential – corresponding to the amount released by 2000 gas burners.	$0.00253m^3/s$ $0.00505m^3/s$ $0.00758m^3/s$ $0.0112m^3/s$
4	Temperature	6^oC	24^oC
5	Salinity	34 - 35 grams of salt per litre of water	32 – 37 parts per thousand

5.3 Typical plume behaviors at varying depths

60 cm

0.5m
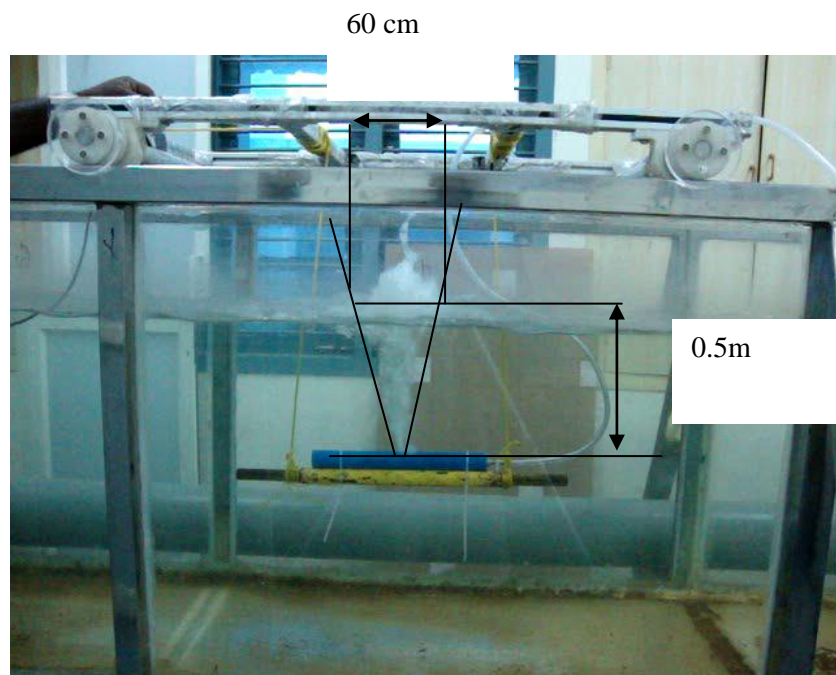
Fig 5.7   : Plume behaviour at
Depth   : 0.5m
Flow Rate   : 0.0112m^3/s

81 cm
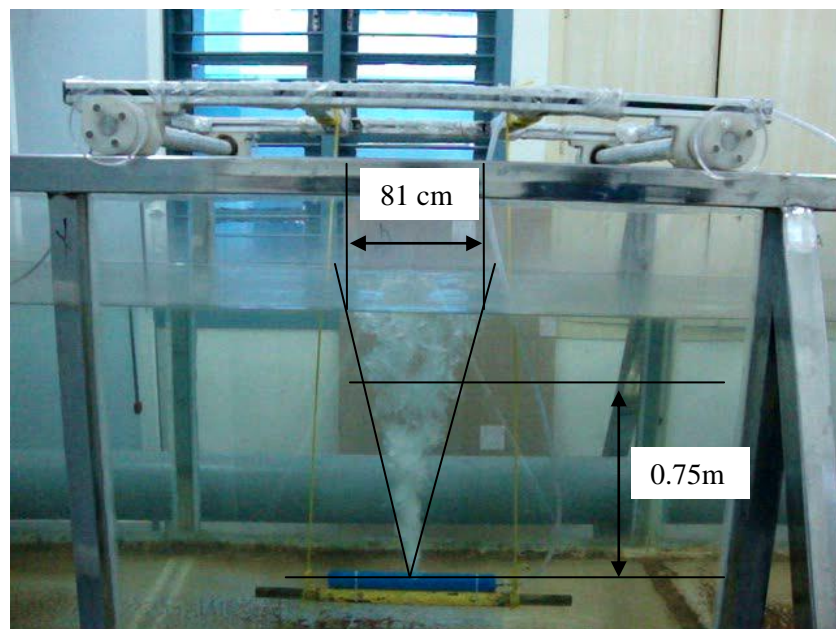
0.75m

Fig 5.8   : Plume behaviour at
Depth   : 0.75m
Flow Rate   : 0.0112m^3/s

104 cm

1.0m
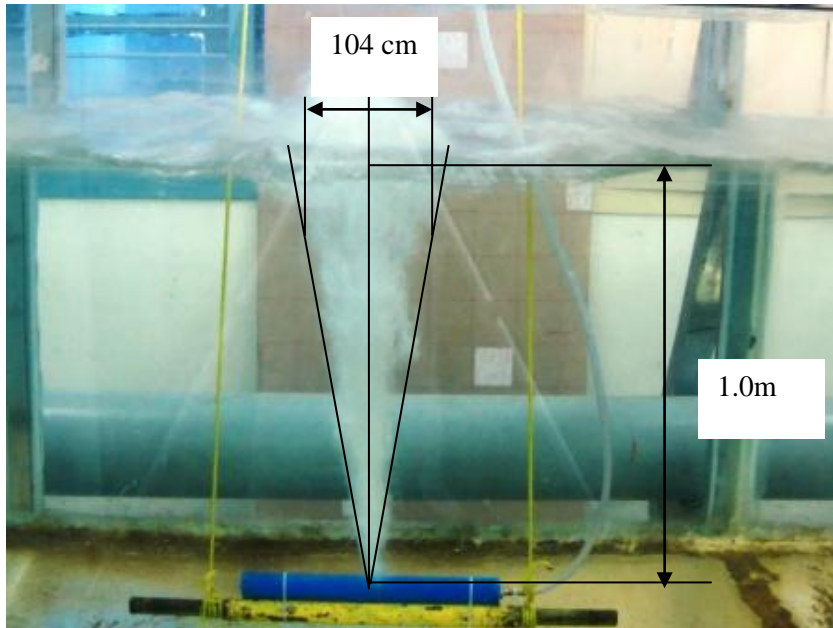
Fig 5.9   : Plume behaviour at
Depth   :1m
Flow Rate   : 0.0112m^3/s

114 cm

1.5 m
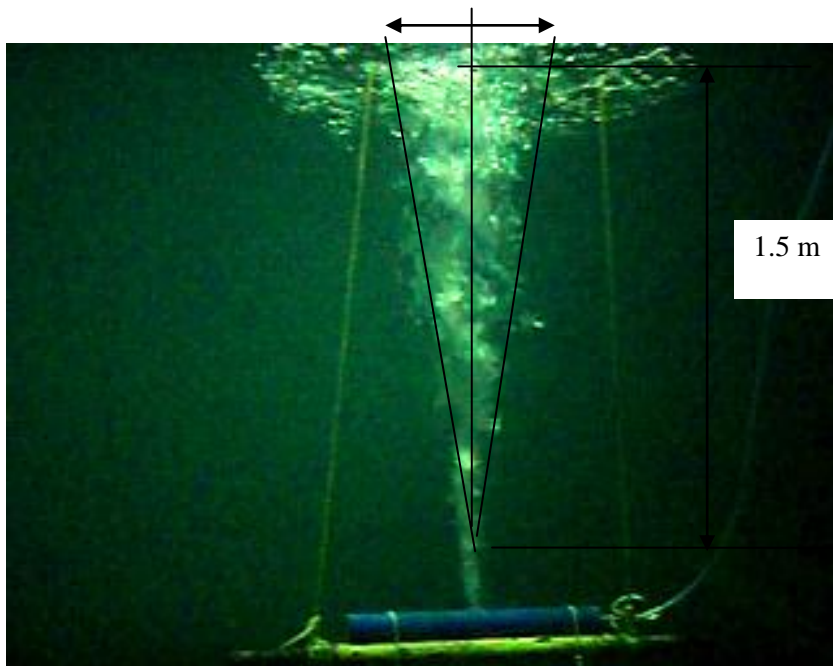
Fig 5.10   : Plume behaviour at
Depth   : 1.5m
Flow Rate   : 0.0112m^3/s

5.4 Typical Plume behaviour at various flow rates

Fig 5.11   : Plume behaviour at
Depth   : 1m
Flow Rate   : $0.00253 m^3/s$

Fig 5.12   : Plume behaviour at
Depth   : 1m
Flow Rate   : $0.00505 m^3/s$

Fig 5.13   : Plume behaviour at
Depth   : 1m
Flow Rate   : $0.00758 m^3/s$
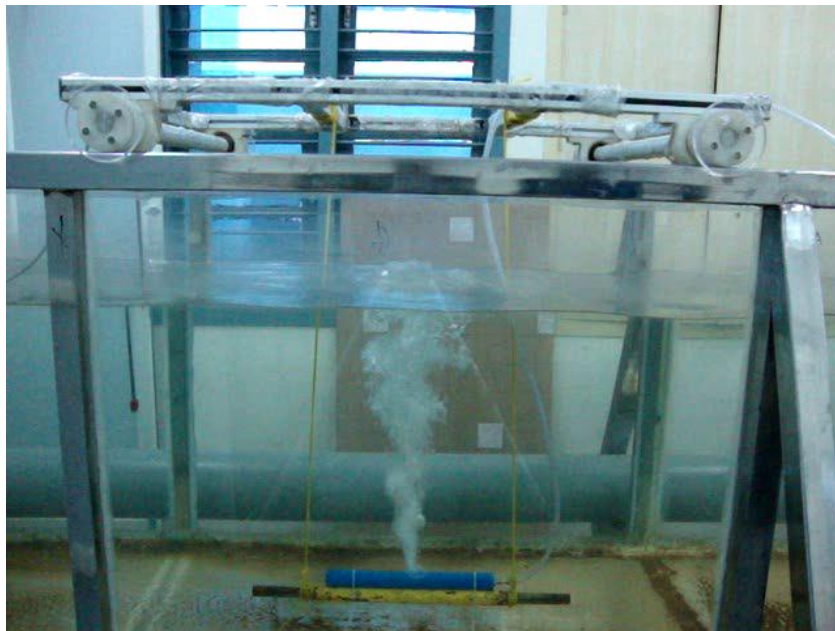
Fig 5.14   : Plume behaviour at
Depth   : 1m
Flow Rate   : $0.0112 m^3/s$

5.5 Experimentation Readings

Table 5.2 Raw readings from Experimentation

S.N	Ho (m)	Gas Flow rate m3/s	Measured Plume Diameter					Avg. Plume Diameter (m)	Avg. Plume Radius (m)	Cone Angle
			Trial 1	Trial 2	Trial 3	Trial 4	Trial 5			
1	0.5	0.00253	0.105	0.095	0.1	0.1	0.1	0.1	0.05	11.4212
2	0.5	0.00505	0.115	0.11	0.12	0.11	0.115	0.115	0.0575	13.1204
3	0.5	0.00758	0.115	0.115	0.12	0.12	0.125	0.12	0.06	13.6854
4	0.5	0.0112	0.125	0.12	0.12	0.12	0.12	0.12	0.06	13.6854
5	0.75	0.00253	0.155	0.15	0.145	0.145	0.155	0.15	0.075	11.4212
6	0.75	0.00505	0.16	0.155	0.155	0.155	0.155	0.156	0.078	11.8748
7	0.75	0.00758	0.155	0.155	0.16	0.155	0.155	0.156	0.078	11.8748
8	0.75	0.0112	0.16	0.165	0.16	0.16	0.165	0.162	0.081	12.328
9	1	0.00253	0.19	0.195	0.2	0.195	0.195	0.195	0.0975	11.1374
10	1	0.00505	0.2	0.195	0.195	0.195	0.195	0.195	0.0975	11.1374
11	1	0.00758	0.205	0.21	0.205	0.21	0.21	0.208	0.104	11.8748
12	1	0.0112	0.21	0.21	0.205	0.21	0.21	0.208	0.104	11.8748
13	1.5	0.00253	0.26	0.265	0.265	0.27	0.26	0.264	0.132	10.058
14	1.5	0.00505	0.265	0.265	0.265	0.27	0.26	0.264	0.132	10.058
15	1.5	0.00758	0.275	0.27	0.27	0.27	0.275	0.272	0.136	10.3612
16	1.5	0.0112	0.29	0.29	0.285	0.29	0.285	0.288	0.144	10.9672

5.6 Data Mining

a. The CART method under Tanagra and R (rpart)

CART (Breiman and al., 1984) is a very popular classification tree (says also decision tree) learning algorithm. CART incorporates all the ingredients of a good learning control: the post-pruning process enables to make the trade-off between the bias and the variance; the cost complexity mechanism enables to "smooth" the exploration of the space of solutions; we can control the preference for simplicity with the standard error rule (SE-rule); etc. Thus, the data miner can adjust the settings according to the goal of the study and the data characteristics. The Breiman's algorithm is provided under different designations in the free data mining tools. Tanagra uses the "C-RT" name. R, through a specific package , provides the "rpart" function.

b. Naive Bayes classifier for continuous predictors

The Naive Bayes classifier is a very popular approach even if it is (apparently) based on an unrealistic assumption: the distributions of the predictors are mutually independent conditionally to the values of the target attribute. The main reason of this popularity is that the method proved to be as accurate as the other well-known approaches such as linear discriminate analysis or logistic regression on the majority of the real dataset.

But an obstacle to the utilization of the naive bayes classifier remains when we deal with a real problem. It seems that we cannot provide an explicit model for its deployment. The interpretation of the model, especially the detection of the influence of each descriptor on the prediction of the classes is impossible.

This assertion is not entirely true. We can extract an explicit model from the naive bayes classifier in the case of discrete predictors (see references). We obtain a linear combination of the binarized predictors. In this write-up, we show that the same mechanism can be implemented for the continuous descriptors. We use the standard Gaussian assumption for the conditional distribution of the descriptors. According to the heteroscedastic assumption or the homoscedastic assumption, we can provide a quadratic model or a linear model. This last one is especially interesting because we obtain a model that we can directly compare to the other linear classifiers (the sign and the values of the coefficients of the linear combination).

c. The ID3 algorithm

The ID3 algorithm can be summarized as follows:

1. Take all unused attributes and count their entropy concerning test samples
2. Choose attribute for which entropy is minimum (or, equivalently, information gain is maximum)
3. Make node containing that attribute

The algorithm is as follows:

ID3 (Examples, Target_Attribute, Attributes)

   a. Create a root node for the tree
   b. If all examples are positive, Return the single-node tree Root, with label = +.

c. If all examples are negative, Return the single-node tree Root, with label = -.

d. If number of predicting attributes is empty, then Return the single node tree Root, with label = most common value of the target attribute in the examples.

e. Otherwise Begin

- A = The Attribute that best classifies examples.
- Decision Tree attribute for Root = A.
- For each possible value, v_i, of A,
  - Add a new tree branch below Root, corresponding to the test A = v_i.
  - Let Examples(v_i) be the subset of examples that have the value v_i for A
  - If Examples(v_i) is empty
  - Then below this new branch add a leaf node with label = most common target value in the examples
  - Else below this new branch add the subtree ID3 (Examples(v_i), Target_Attribute, Attributes – {A})
  - End
  - Return Root

d. C4.5 Algorithm

C4.5 is an algorithm used to generate a decision tree developed by Ross Quinlan. C4.5 is an extension of Quinlan's earlier ID3 algorithm. The decision trees generated by C4.5 can be used for classification, and for this reason, C4.5 is often referred to as a statistical classifier.

C4.5 builds decision trees from a set of training data in the same way as ID3, using the concept of information entropy. The training data is a set $S = S_1, S_2, \ldots$ of already classified samples. Each sample $S_i = x_1, x_2, \ldots$ is a vector where $x_1, x_2, \ldots$ represent attributes or features of the sample. The training data is augmented with a vector $C = C_1, C_2, \ldots$ where $C_1, C_2, \ldots$ represent the class to which each sample belongs.

At each node of the tree, C4.5 chooses one attribute of the data that most effectively splits its set of samples into subsets enriched in one class or the other. Its criterion is the normalized information gain (difference in entropy) that results from choosing an attribute for splitting the data. The attribute with the highest normalized information gain is chosen to make the decision. The C4.5 algorithm then recurses on the smaller sub lists.

e. K-nearest neighbour algorithm

In pattern recognition, the **k-nearest neighbor algorithm** (*k*-NN) is a method for classifying objects based on closest training examples in the feature space. *k*-NN is a type of instance-based learning, or lazy learning where the function is only approximated locally and all computation is deferred until classification. The *k*-nearest neighbor algorithm is amongst the simplest of all machine learning algorithms: an object is classified by a majority vote of its neighbors, with the object being assigned to the class most common amongst its *k* nearest neighbors (*k* is a positive integer, typically small). If $k = 1$, then the object is simply assigned to the class of its nearest neighbor.

The same method can be used for regression, by simply assigning the property value for the object to be the average of the values of its *k* nearest neighbors. It can be useful to weight the contributions of the neighbors, so that the nearer neighbors contribute more to the average than the more distant ones. (A common weighting scheme is to give each neighbor a weight of $1/d$, where *d* is the distance to the neighbor. This scheme is a generalization of linear interpolation.)

The neighbors are taken from a set of objects for which the correct classification (or, in the case of regression, the value of the property) is known. This can be thought of as the training set for the algorithm, though no explicit training step is required. The *k*-nearest neighbor algorithm is sensitive to the local structure of the data.

Nearest neighbor rules in effect compute the decision boundary in an implicit manner. It is also possible to compute the decision boundary itself explicitly, and to do so in an efficient manner so that the computational complexity is a function of the boundary complexity.

f. Multilayer perceptron

A multilayer perceptron (MLP) is a feed forward artificial neural network model that maps sets of input data onto a set of appropriate output. An MLP consists of multiple layers of nodes in a directed graph, with each layer fully connected to the next one. Except for the input nodes, each node is a neuron (or processing element) with a nonlinear activation function. MLP utilizes a supervised learning technique called back propagation for training

the network. MLP is a modification of the standard linear perceptron and can distinguish data that is not linearly separable, Random forest.

g. Random forest (or random forests) is an ensemble classifier that consists of many decision trees and outputs the class that is the mode of the classes output by individual trees. The algorithm for inducing a random forest was developed by Leo Breiman and Adele Cutler, and "Random Forests" is their trademark. The term came from random decision forests that were first proposed by Tin Kam Ho of Bell Labs in 1995. The method combines Breiman's "bagging" idea and the random selection of features, introduced independently by Ho and Amit and Geman in order to construct a collection of decision trees with controlled variation.

The selection of a random subset of features is an example of the random subspace method, which, in Ho's formulation, is a way to implement stochastic discrimination proposed by Eugene Kleinberg.

Table 5.3 Typical dataset from experimentation

S.N	Sea depth Ho (m)	Gas flow rate (Kg/s)	Plume radius (m)
1	0.5	0.00258	0.02
2	0.5	0.00505	0.023
3	0.5	0.00758	0.024
4	0.5	0.0112	0.024
5	0.75	0.00258	0.025
6	0.75	0.00505	0.026
7	0.75	0.00758	0.026
8	0.75	0.0112	0.027
9	1	0.00258	0.03
10	1	0.00505	0.03
11	1	0.00758	0.031
12	1	0.0112	0.031
13	1.5	0.00258	0.033
14	1.5	0.00505	0.033
15	1.5	0.00758	0.034
16	1.5	0.0112	0.036

h. Selection of Data mining method

Table 5.4 Comparison of Classification Algorithms for Gas Leakage dataset

S.No	Algorithm	Error Rate
1	C4.5	0.7500
2	ID3	0.8750
3	C-RT	0.8750
4	PLS	-
5	CS-MC4	0.7500
6	KNN	0.3125
7	SVM	-
8	**RND TREE**	**0.0000**
9	NAIVE BAYES	0.7500
10	**MLP**	**0.0000**

Rnd Tree algorithm is given below.

Decision Tree for Rand Tree classifier

If (Ho < 0.8750)

{ If (flow < 0.0038)

{ If (Ho < 0.6250)

{ then Plume = 0.02M (100.00 % of 1 examples)) }

//Ho >= 0.6250 then Plume = 0.025M (100.00 % of 1 examples)

else

{ If (flow >= 0.0038)

Ho < 0.6250

flow < 0.0063 then Plume = 0.023M (100.00 % of 1 examples)

flow >= 0.0063 then Plume = 0.024M (100.00 % of 2 examples)

Ho >= 0.6250

flow < 0.0094 then Plume = 0.026M (100.00 % of 2 examples)

flow >= 0.0094 then Plume = 0.027M (100.00 % of 1 examples)

Ho >= 0.8750

Ho < 1.2500

flow < 0.0063 then Plume = 0.03M (100.00 % of 2 examples)

flow >= 0.0063 then Plume = 0.031M (100.00 % of 2 examples)

Ho >= 1.2500

flow < 0.0063 then Plume = 0.033M (100.00 % of 2 examples)

flow >= 0.0063

flow < 0.0094 then Plume = 0.034M (100.00 % of 1 examples)

flow >= 0.0094 then Plume = 0.036M (100.00 % of 1 examples)

Table 5.5 Plume radius- extrapolated

| S.N	Sea depth Ho (m)	Gas flow rate (Kg/s)	Plume radius (m)
1	0.5	0.00258	0.02
2	0.5	0.00505	0.023
3	0.5	0.00758	0.024
4	0.5	0.0112	0.024
5	0.75	0.00258	0.025
6	0.75	0.00505	0.026
7	0.75	0.00758	0.026
8	0.75	0.0112	0.027
9	1	0.00258	0.03
10	1	0.00505	0.03
11	1	0.00758	0.031
12	1	0.0112	0.031
13	1.5	0.00258	0.033
14	1.5	0.00505	0.033
15	1.5	0.00758	0.034
16	1.5	0.0112	0.036

Tan α= opp.side/adjacent side (Radians)

Radians to degree conversion:

1 Degree= (radians)*(180/ π)

So for S.No 1

Tan α= opp.side/adjacent side (Radians)

   = (plume radius*2)/Ho

   = (0.02*2)/0.5

   = 0.04/0.5

   = 0.08 Radians

Radians to Degree conversion:

1 Degree = (radians)*(180/ π)

Tan α = (0.08)*(180/3.14)

Tan   α = 4.58599

If we calculate Tan-1 also it gives wrong result.

α = Tan^{-1}(4.58599)

α   = 77.6988

Table 5.6 Consolidated readings based on which the graphs are plotted

S.N	Ho (m)	Flow rate (m³/s)	Radius (m)	Centre-line velocity (m/s)
1	0.5	0.00253	0.05	5
2	0.5	0.00505	0.0575	7.2
3	0.5	0.00758	0.06	9.4
4	0.5	0.0112	0.06	11.1
5	0.75	0.00253	0.075	4.4
6	0.75	0.00505	0.078	5.6
7	0.75	0.00758	0.078	7.8
8	0.75	0.0112	0.081	9.9
9	1	0.00253	0.0975	3.9
10	1	0.00505	0.0975	4.8
11	1	0.00758	0.104	6.6
12	1	0.0112	0.104	7.43
13	1.5	0.00253	0.132	3.6
14	1.5	0.00505	0.132	4.4
15	1.5	0.00758	0.136	5.3
16	1.5	0.0112	0.144	6.12

5.7 Experimentation Graphs

5.7.1 Impact of Gas flow rate on Centreline velocity
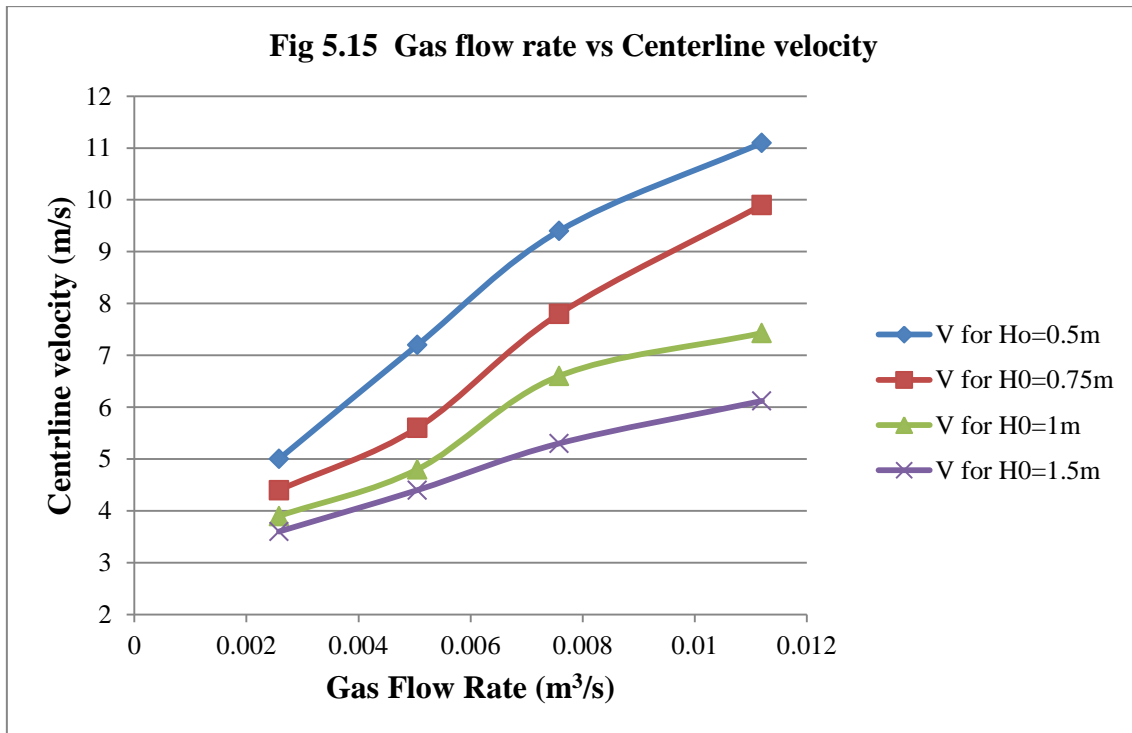
Fig 5.15 Gas flow rate vs Centerline velocity

Gas flow rate and centreline velocity for various depths for Arabian Sea conditions

Vg (m3/s)	V for Ho=0.5m	V for H0=0.75m	V for H0=1m	V for H0=1.5m
0.00253	5	4.4	3.9	3.6
0.00505	7.2	5.6	4.8	4.4
0.00758	9.4	7.8	6.6	5.3
0.0112	11.1	9.9	7.43	6.12

At a particular Depth of Leak (Ho), the centreline velocity (V) of the plume is marginally increasing with respect to gas flow rate (Vg).

At constant Ho, V α Vg

For the lesser depth of leak the change in flow rate has more effect on centerline velocity of the plume when compared to higher depth of leak scenario.

5.7.2 Impact of Gas flow rate on Plume radius

Fig: 5.16 Gas flow rate vs Plume radius
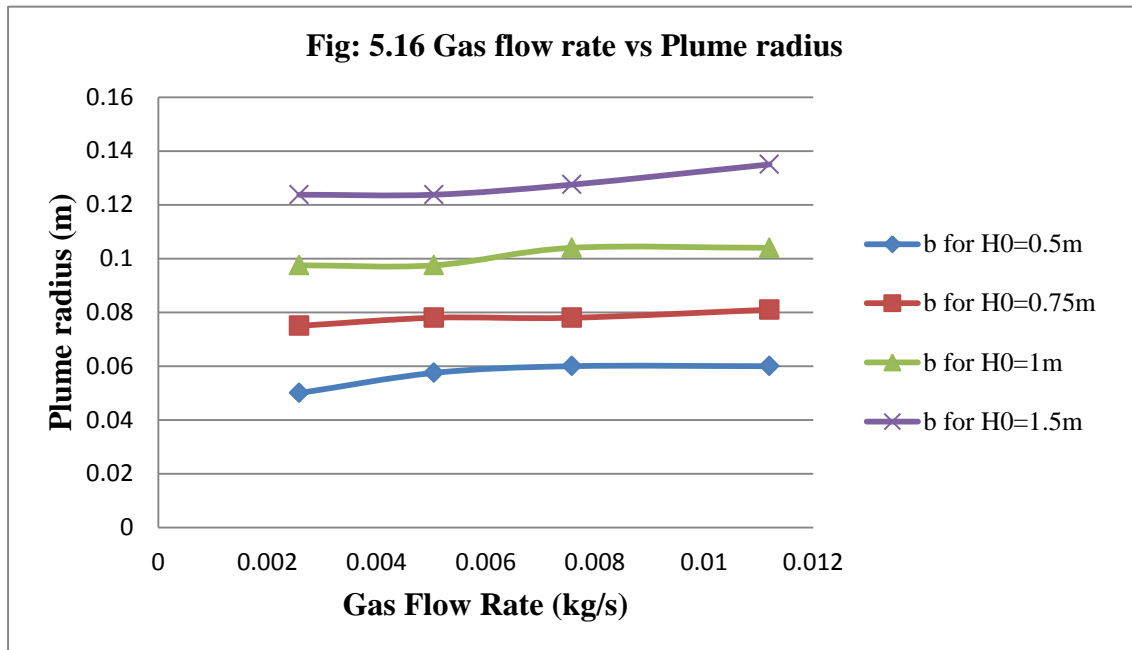
Gas flow rate and plume radius for various depths for Arabian Sea conditions

| Vg (m3/s)	b for H0=0.5m	b for H0=0.75m	b for H0=1m	b for H0=1.5m
0.00253	0.05	0.075	0.0975	0.12375
0.00505	0.0575	0.078	0.0975	0.12375
0.00758	0.06	0.078	0.104	0.1275
0.0112	0.06	0.081	0.104	0.135

The gas flow rate does not have significant effect on plume radius. At a given flow rate, there is a significant increase in the plume radius with increasing depth of leak. This is because as the depth increases the surface tension acting on the bubble plume also increases. The maximum difference in radius is observed at higher depth.

At constant Vg, b α Ho

5.7.3 Impact of Depth of Leak on Centreline velocity

**Fig 5.17 Depth of Leak vs Centerline velocity**
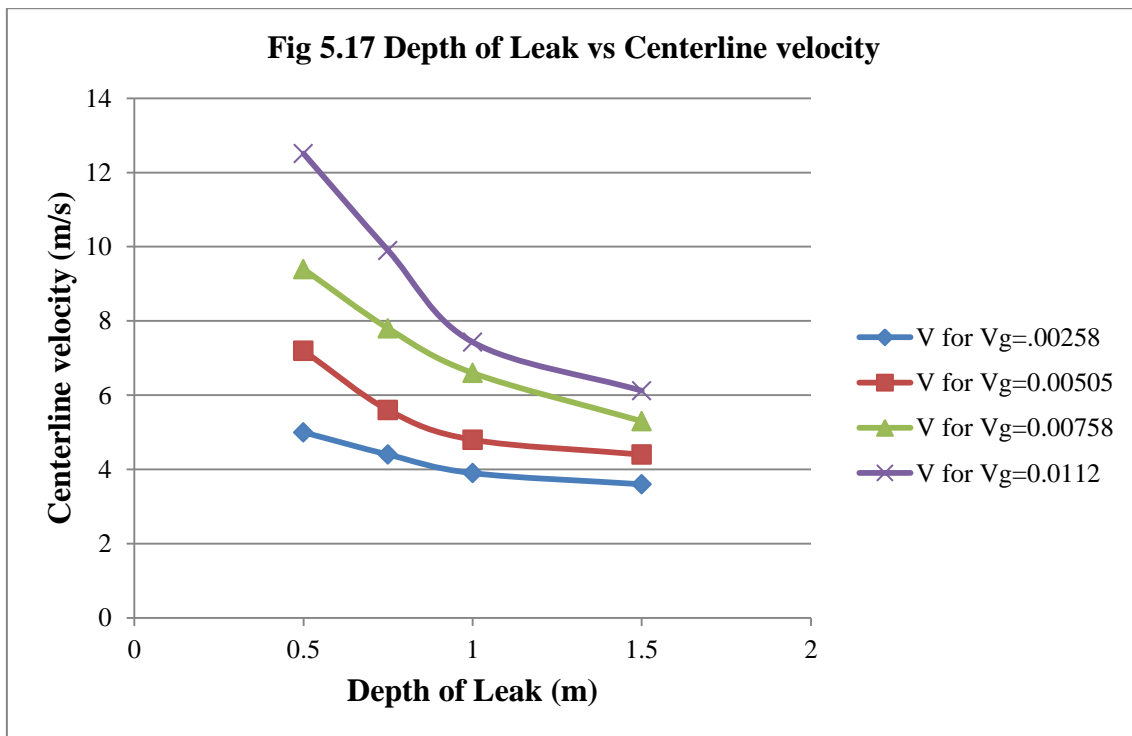
Depth of Leak and centreline velocity for various flow rates for Arabian Sea conditions

Ho(m)	V for Vg=0.00253	V for Vg=0.00505	V for Vg=0.00758	V for Vg=0.0112
0.5	5	7.2	9.4	11.1
0.75	4.4	5.6	7.8	9.9
1	3.9	4.8	6.6	7.43
1.5	3.6	4.4	5.3	6.12

As the ocean depth increases (flow distance also increases), the frictional forces acting along the length of flow also decrease the velocity of flow thus leading to gradual decrease in flow velocity with increasing depth of leak.

Velocity is also dependent on the gas flow rate i.e., as the flow rate increases, the velocity also increases. The hydrostatic pressure acting on the plume (bubbles) increases with depth but due to surface tension the bubble breaks and a balance is maintained for the plume to flow.

5.7.4 Impact of Depth of Leak on Plume radius

Fig 5.18 Depth of Leak vs Plume radius
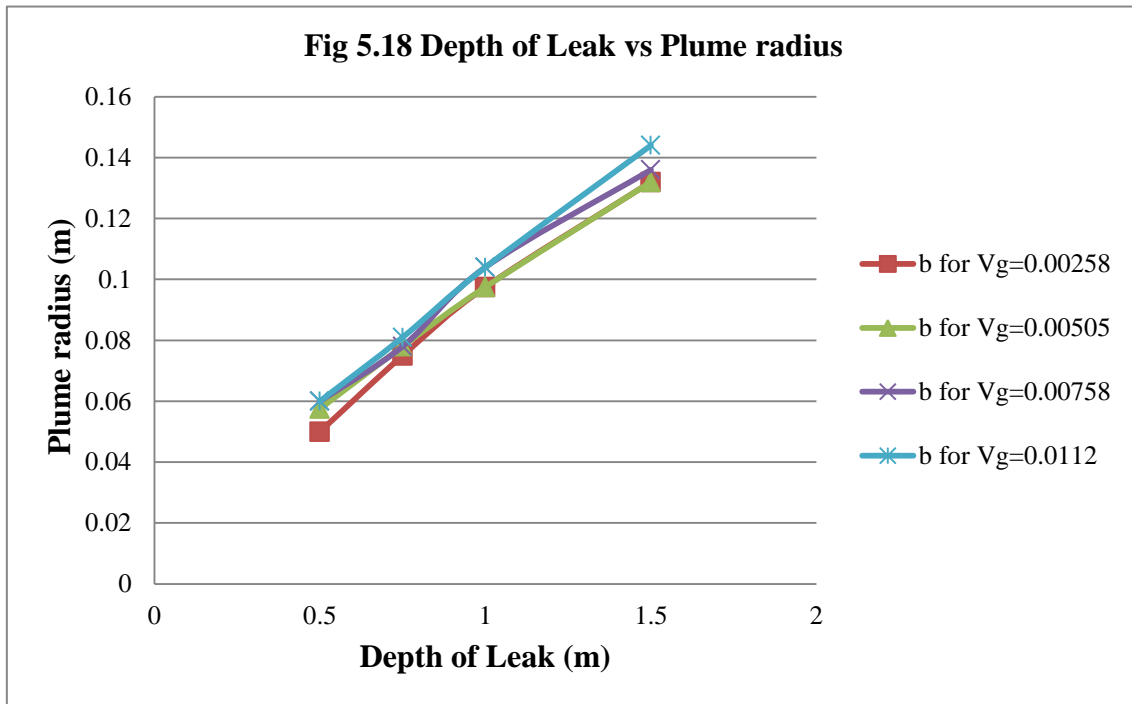
Depth of Leak and plume radius for various flow rates for Arabian Sea conditions

| Ho(m)	b for Vg=0.00253	b for Vg=0.00505	b for Vg=0.00758	b for Vg=0.0112
0.5	0.05	0.0575	0.06	0.06
0.75	0.075	0.078	0.078	0.081
1	0.0975	0.0975	0.104	0.104
1.5	0.132	0.132	0.136	0.144

The initial pressure of the gas released from the pipe is high, the gas coming out from the pipe expands thus the plume diameter increases as it advances. Also the hydrostatic pressure acting on the plume bubbles surface decreases as the plume raises in the water which allows the plume to further diverge its flow. As the flow rate is increased, the pressure of flow also increases which has very small effect on the diameter of plume. The maximum difference in diameter of plume was observed to be 0.0112m at a depth of 1.5m in comparision with flow rates of 0.00253 and 0.0112m^3/s. Hence when compared to flow rate, the depth of release has got mariginal impact on the diameter of the plume.

5.8 Key findings and conclusions from experimentation

S.N	Parameter varied	Range	Key findings
1	Water depth Height of water column (Ocean depth)	500 - 1500m	Plume radius marginally increases with water depth.
2	Leakage/ flow rate/ release rate	0.00253-0.0112m³/s	There is less effect of flow rate on plume radius.
3	Sea temperature	24^{0}C	Sea temperature does not have any effect on plume behavior.
4	Salinity	32 – 37 parts per thousand	Salinity does not have any effect on plume behavior.

5.9 Chapter Summary

Simple cone models assume either that the bubble plume has a cone of angle θ, or, equivalently, that the radius at the surface is a fixed proportion of the depth: i.e. b (z) =z tan (θ/2) as illustrated in Fig 2.1 which is reproduced below.
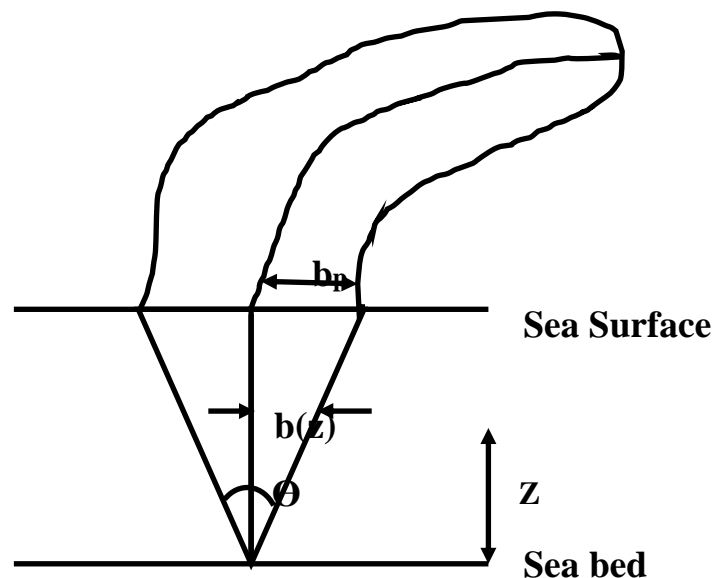
It is assumed that θ, and hence tan θ/2, are fixed parameters which do not vary significantly with release rate or depth. The value of the model constants used varies significantly. The cone angle is established between 10-12°. Lower values closely match that of 10° that is given by **Wilson, 1988** [25] **and Milgram and Erb, 1984** [15]. This cone angle is defined as

that of the subsea plume and does not include the effect of radial flow, which is known to occur near the sea surface.

In summary, the plume model established through IIT experimentation for Arabian Sea conditions very well matches the Plume model established by Fanneløp and Sjøen (1980) [7] and the plume measurements published by Milgram (1983) [17] for North Sea and Norwegian Sea conditions.

Implication of results on safety sensitive studies and risk assessment.

Higher radius of the plume indicates wider cover area and hence a higher fire and explosion risk. A large area further increases the possibility of coming in contact with the ignition source. Whereas the radius of plume establised by experimentation is in the range of 10-12° which represents low Hazard zone.

6. MODELS FOR RESEARCH PROBLEM'S COMPETENCE

6.1 Empirical constructs

The depth of the Plume source (sub-sea pipeline leak source) was determined based on the Mean depth of Arabian Sea (Source: NIOT web site) considering the fact that this is the average depth at which deep sea Exploration and Production (E&P) activities are likely to intensify in the near future.


Maximum depth	: 750 m
Mean depth	: 90 m
Sea temperature	: 6 - 17° C

Maximum depth	: 4652 m
Mean depth	: 2734 m
Sea temperature	: 24 - 29° C

6.2 Comparing North Sea and Norwegian Sea experimentation results with IIT experimentation results - Plume variables as function of gas flow rate for different ocean depths.

6.2.1 Gas flow rate and centreline velocity for various depths for North Sea and Norwegian Sea conditions

Fig 6.1 Gas flow rate vs Centerline velocity
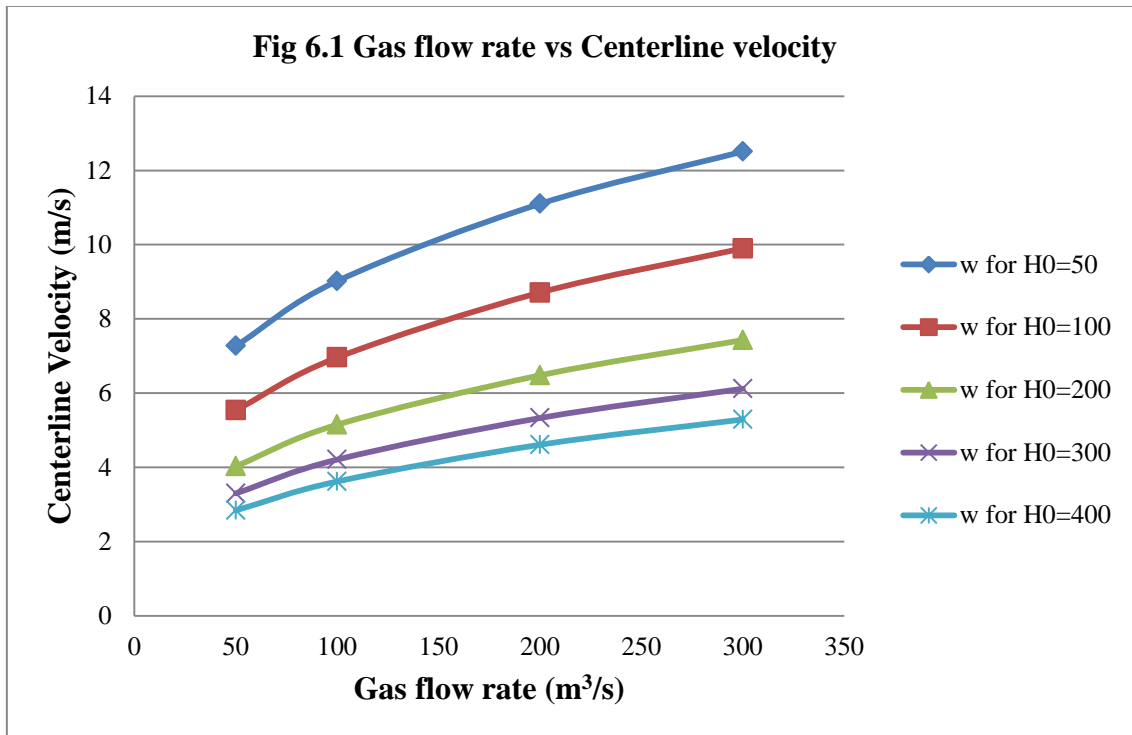
V_g(kg/s)	w for H_0= 50	w for H_0= 100	w for H_0= 200	w for H_0= 300	w for H_0= 400
50	7.27	5.54	4.03	3.3	2.84
100	9.02	6.96	5.15	4.21	3.62
200	11.1	8.71	6.48	5.33	4.61
300	12.5	9.9	7.43	6.12	5.29

6.2.2 Gas flow rate and centreline velocity for various depths for Arabian Sea conditions
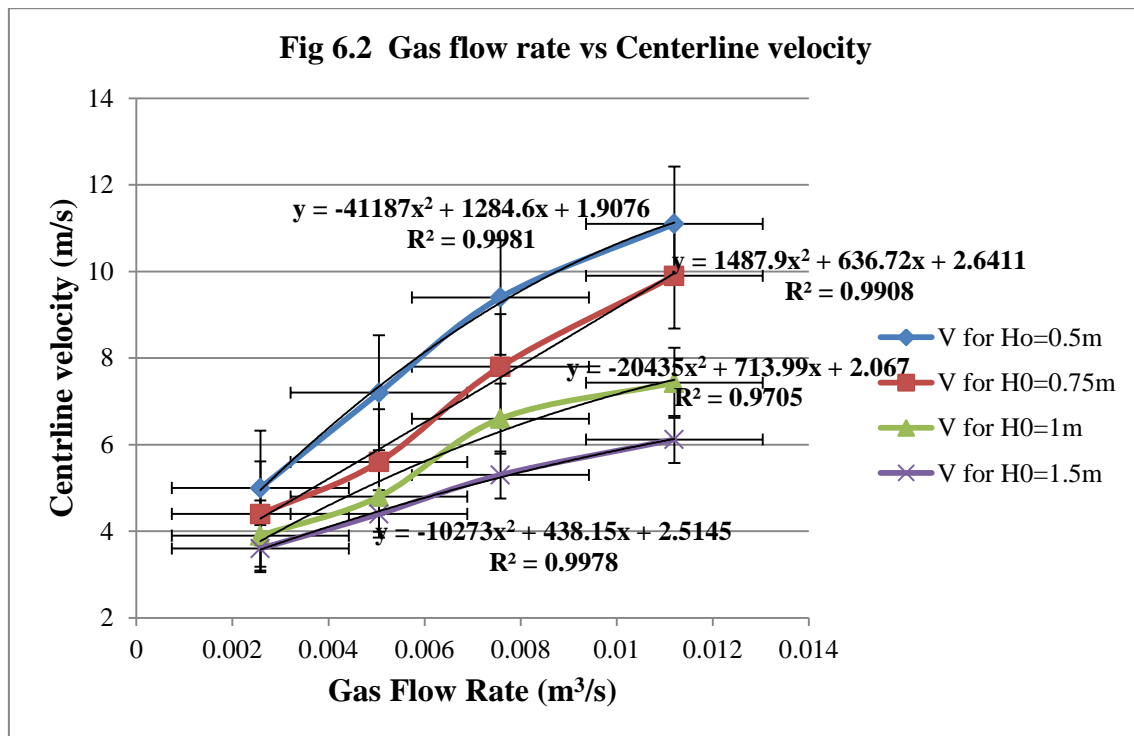
Fig 6.2 Gas flow rate vs Centerline velocity

$y = -41187x^2 + 1284.6x + 1.9076$
$R^2 = 0.9981$

$y = 1487.9x^2 + 636.72x + 2.6411$
$R^2 = 0.9908$

$y = -20435x^2 + 713.99x + 2.067$
$R^2 = 0.9705$

$y = -10273x^2 + 438.15x + 2.5145$
$R^2 = 0.9978$

- V for Ho=0.5m
- V for H0=0.75m
- V for H0=1m
- V for H0=1.5m

Vg (m3/s)	V for Ho=0.5m	V for H0=0.75m	V for H0=1m	V for H0=1.5m
0.00253	5	4.4	3.9	3.6
0.00505	7.2	5.6	4.8	4.4
0.00758	9.4	7.8	6.6	5.3
0.0112	11.1	9.9	7.43	6.12

6.2.3 Gas flow rate and plume diameter for various depths for North Sea and Norwegian Sea conditions

Fig 6.3 Gas flow rate vs Plume diameter
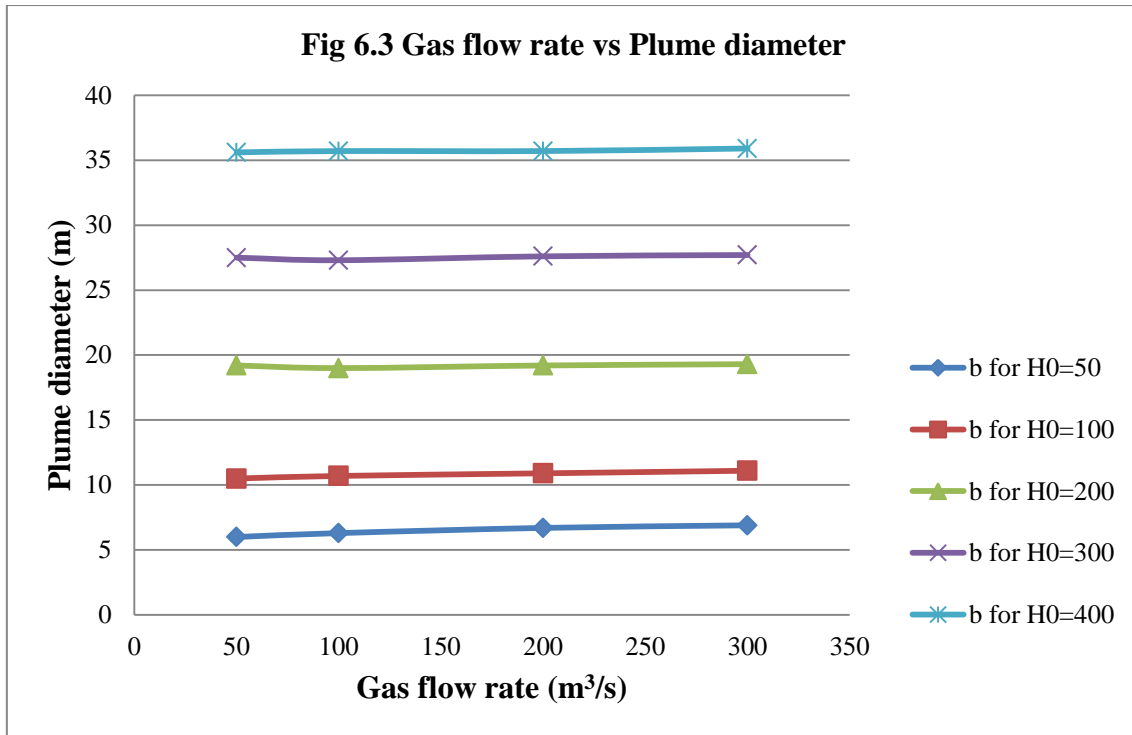
Vg (kg/s)	b for H0=50	b for H0=100	b for H0=200	b for H0=300	b for H0=400
50	6	10.5	19.2	27.5	' 35.6 '
100	6.3	10.7	19	27.3	35.7
200	6.7	10.9	19.2	27.6	35.7
300	6.9	11.1	19.3	27.7	35.9

6.2.4 Gas flow rate and plume radius for various depths for Arabian Sea conditions
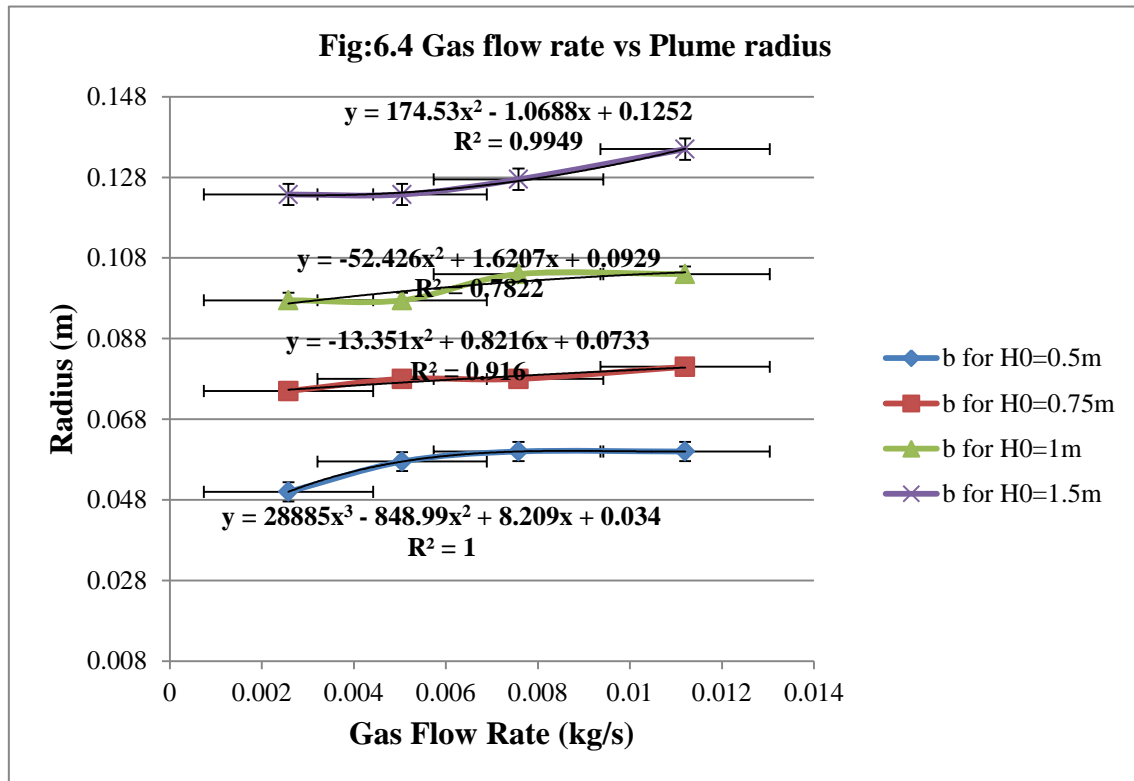
Fig:6.4 Gas flow rate vs Plume radius

$$y = 174.53x^2 - 1.0688x + 0.1252$$
$$R^2 = 0.9949$$

$$y = -52.426x^2 + 1.6207x + 0.0929$$
$$R^2 = 0.7822$$

$$y = -13.351x^2 + 0.8216x + 0.0733$$
$$R^2 = 0.916$$

$$y = 28885x^3 - 848.99x^2 + 8.209x + 0.034$$
$$R^2 = 1$$

Legend:
- b for H0=0.5m
- b for H0=0.75m
- b for H0=1m
- b for H0=1.5m

X-axis: Gas Flow Rate (kg/s)
Y-axis: Radius (m)

Vg (m3/s)	b for H0=0.5m	b for H0=0.75m	b for H0=1m	b for H0=1.5m
0.00253	0.05	0.075	0.0975	0.12375
0.00505	0.0575	0.078	0.0975	0.12375
0.00758	0.06	0.078	0.104	0.1275
0.0112	0.06	0.081	0.104	0.135

6.2.5 Ocean depth and centreline velocity for various flow rates for North Sea and Norwegian Sea conditions

Fig 6.5 Ocean depth vs centerline velocity
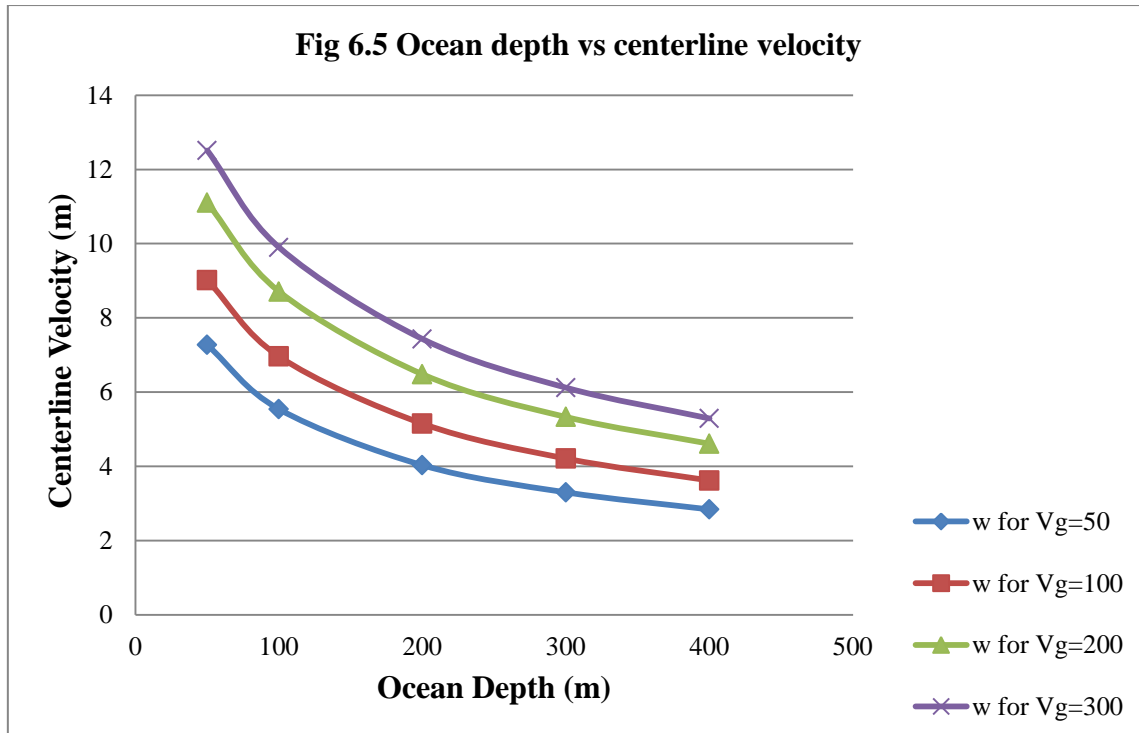
Ho(m)	w for Vg=50	w for Vg=100	w for Vg=200	w for Vg=300
50	7.27	9.02	11.1	12.51
100	5.54	6.96	8.71	9.9
200	4.03	5.15	6.48	7.43
300	3.3	4.21	5.33	6.12
400	2.84	3.62	4.61	5.29

6.2.6 Ocean depth and centreline velocity for various flow rates for Arabian Sea conditions
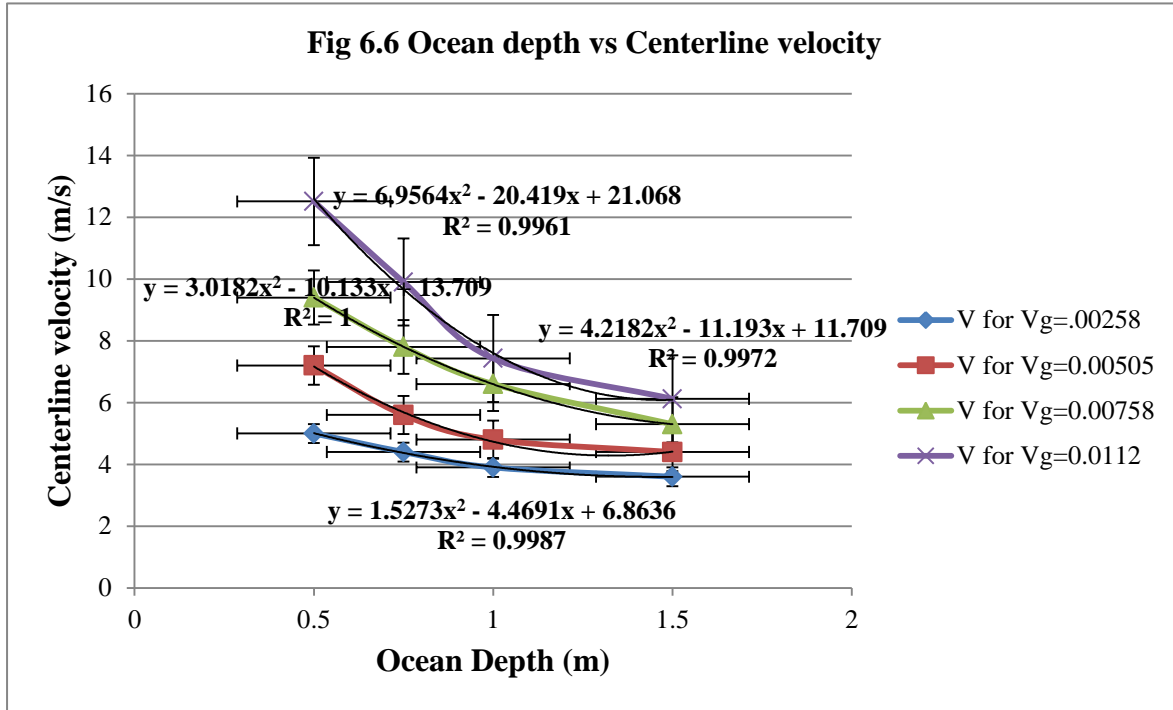
Fig 6.6 Ocean depth vs Centerline velocity

Ho(m)	V for Vg=0.00253	V for Vg=0.00505	V for Vg=0.00758	V for Vg=0.0112
0.5	5	7.2	9.4	11.1
0.75	4.4	5.6	7.8	9.9
1	3.9	4.8	6.6	7.43
1.5	3.6	4.4	5.3	6.12

6.2.7 Ocean depth and plume diameter for various flow rates for North Sea and Norwegian Sea conditions

Fig 6.7 Ocean depth vs Plume diameter
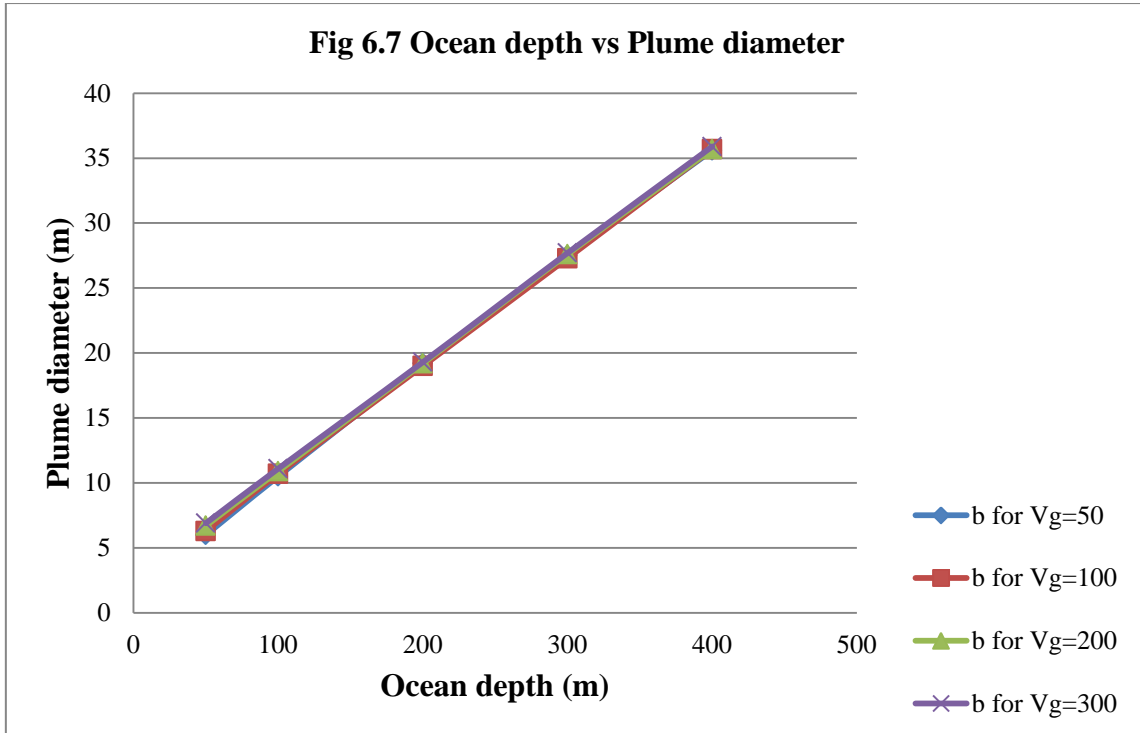
Ho(m)	b for Vg=50	b for Vg=100	b for Vg=200	b for Vg=300
50	6	6.3	6.7	6.9
100	10.5	10.7	10.9	11.1
200	19.2	19	19.2	19.3
300	27.5	27.3	27.6	27.7
400	35.6	35.7	35.7	35.9

6.2.8 Ocean depth and plume radius for various flow rates for Arabian Sea conditions

Fig 6.8 Ocean depth vs Plume radius

$y = -0.0058x^2 + 0.0961x + 0.0131$
$R^2 = 0.9997$

$y = -0.016x^2 + 0.1096x + 0.008$
$R^2 = 0.9946$

$y = -0.0107x^2 + 0.096x + 0.0121$
$R^2 = 1$

$y = -0.0255x^2 + 0.133x - 0.0102$
$R^2 = 1$

Ho(m)	b for Vg=0.00253	b for Vg=0.00505	b for Vg=0.00758	b for Vg=0.0112
0.5	0.05	0.0575	0.06	0.06
0.75	0.075	0.078	0.078	0.081
1	0.0975	0.0975	0.104	0.104
1.5	0.132	0.132	0.136	0.144

6.3. Corroboration of experimentation results with CFD modelling

6.3.1 Computational Fluid Dynamics (CFD)

Superficial gas velocity, pressure, bubble size are the salient parameters that are needed to be studied with respect to Plume Modeling. Using CFD (Computational fluid dynamics), this study shall be done with a focus on the bubble size distribution.

Among available simulation approaches, the volume of fluid (VOF) (Hirt et al., 1981) is one of the most well-known methods for volume tracking in which the motion of all phases is modelled by solving a single set of transport equations with appropriate jump boundary conditions at the interface (Delnoij et al., 1997; Krishna et al., 1999). The only drawback of VOF method is the so-called artificial (or numerical) coalescence of gas bubbles which occurs when their mutual distances is less than the size of the computational cell, which also makes this approach memory intensive for simulation of dispersed multiphase flows in large equipment (Ranade 2002).

The current simulation involves modeling of bubbles rising through a bubble chamber at different flow rates and different free surface height. The size of the bubble at the free surface is studied. Commercial coded Fluent (14.0) simulation software is used , meshing is done using ICEM CFD and structured mesh with a fine grid is used to bring about a balance in the solution accuracy and as well as the load on the computation. VOF model was used to track the interface between the two phases i.e. liquid and gas phase. Computationally 3D VOF simulations are least expensive when compared to other schemes available. The CFD results are compared with the experimental results and they were in coherence with minor exceptions.

a. Computational methods and models

Computational fluid dynamics and governing equations:

Instantaneous flow velocity and pressure can be obtained by solving the Navier-stokes equation. This technique can be used to capture the physics of the gas propagating through the fluid phase, and the different influences on these gases due to depth, flow rate etc.

b. Governing equations and formulations

Choice of Governing Equations:

At the outset, an important decision should be taken with regard to the use of the governing equations; type of flow whether laminar or turbulent; boundary conditions and other conditions pertaining to computation. The equations governing the flow over a rotating domain in general are given below.

Continuity:
$$\frac{\partial \rho}{\partial t} + \frac{\partial}{\partial x_j}(\rho U_j) = 0$$

Momentum or Navier- Stokes Equation: $\frac{\partial}{\partial t}(\rho U_i) + \frac{\partial}{\partial x_j}(\rho U_i U_j) = -\frac{\partial p}{\partial x_i} + \frac{\partial \tau_{ij}}{\partial x_j} + \rho f_i$

Energy Equation:
$$\frac{\partial}{\partial t}(\rho h) + \frac{\partial}{\partial x_j}(\rho U_j h) = \frac{\partial p}{\partial t} + U_j \frac{\partial p}{\partial x_j} + \tau_{ij}\frac{\partial U_i}{\partial x_j} - \frac{\partial q_i}{\partial x_i}$$

Equation of State: $p = \rho RT$

c. Turbulence model

The turbulence in the continuous phase has been modeled using a modified *k-ε* turbulence model available in FLUENT 14.0, which is widely used turbulence model to simulate turbulence eddies. This model accounts for the transport not only of the turbulence velocity scale but also of the length scale. It employs a transport equation for the length scale that allows the length scale distribution to be determined even in complex flow situations like in bubble column. It is the simplest model that promise success for flows for which the length scale cannot be prescribed empirically in an easy way.

d. Boundary condition

A constant mass flow rate the inlet, the mass flow rate depended on the data from the experimental setup. Turbulent variables were set by specifying the turbulence intensity and hydraulic diameter, turbulence intensity of 10 % was specified at the inlet, the hydraulic diameter according the nominal size of the aperture. A constant pressure outlet at atmospheric pressure was set at the outlet or free surface. Operation pressure was at 1 atmosphere.

e. Volume fraction equation

The tracking of the interface between the gas (in this case Air) and liquid is accomplished by the solution of a continuity equation for the volume fraction of gas, which is:

$$\frac{\partial}{\partial t}(\alpha_G) + v\nabla.\alpha_G$$

The volume fraction equation is not solved for the liquid; the liquid volume fraction is computed based on the following constraint:

$$\alpha_G + \alpha_L = 1$$

Where α_G and α_L is the volume fraction of gas and liquid phase respectively. The liquid phase is considered as the primary phase and the gas as the secondary phase. The gas regions are patched using the adapt function in the CFD software, the free surface and the inlet regions are patch with a volume fraction of 0.9. Back flow volume fraction at the out let is 1 since air exists consistently above the free surface.

f. Surface Tension

The surface tension model in FLUENT is the Continuum Surface Force (CSF) model proposed by Brackbill et al. (FLUENT 14.0 Manual). With this model, the addition of surface tension to the VOF calculation results in a source term in the momentum equation.

g. Differencing Schemes

In order to minimize numerical diffusion, the first order up-wind differencing scheme is applied for the solution of momentum equation. Higher order scheme (3rd order QUICK) has given similar results. The Pressure-Implicit with Splitting of Operators (PISO) pressure–velocity-coupling scheme, part of the simple family of algorithms, is used for the pressure–velocity-coupling scheme, which is recommended for usual transient calculations. Using PISO allows for a rapid rate of convergence without any significant loss of accuracy. Pressure is discretized with a PRESTO scheme. Other schemes (linear or second-order schemes) lead to strong divergence or to slow convergence (Body force weighted scheme). Segregated algorithms converge poorly unless partial equilibrium of pressure gradient and body forces is taken into account. FLUENT provides an optional "implicit body force"

treatment that can account for this effect, making the solution more robust. The volume fraction equation for gas was solved using an explicit time-marching scheme and the maximum allowed Courant number was set to 0.25. Under relaxation factor used for pressure and momentum were 0.6 and 0.4 respectively. For turbulence parameters, intensity and hydraulic diameter specification was used. A typical value of time step 10e-2 s was used throughout the simulations. The solution is converged in less than fifty iterations at each time step. A simulation time of 3 seconds is used for all of the three-dimensional simulations respectively.

h. Meshing
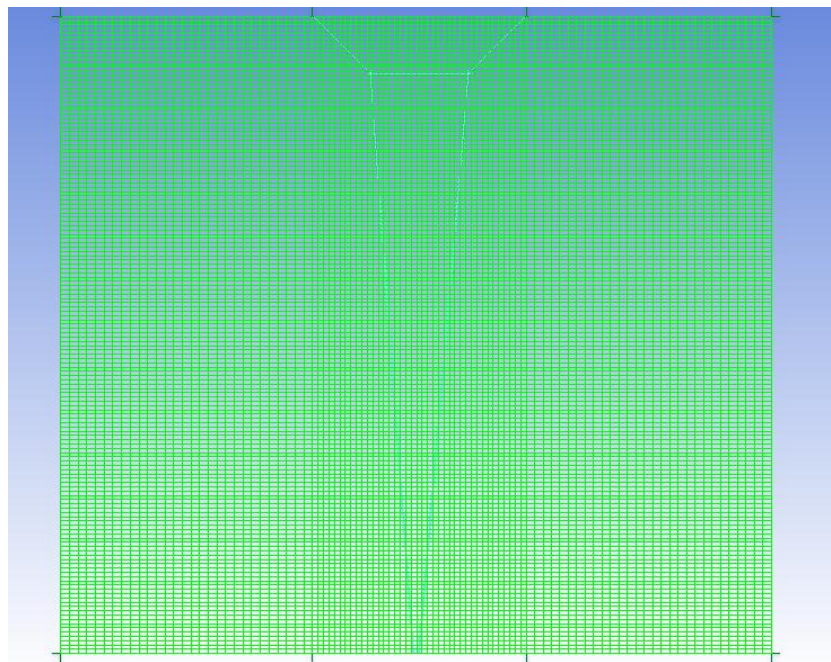

Fig 6.9 Typical CFD meshing
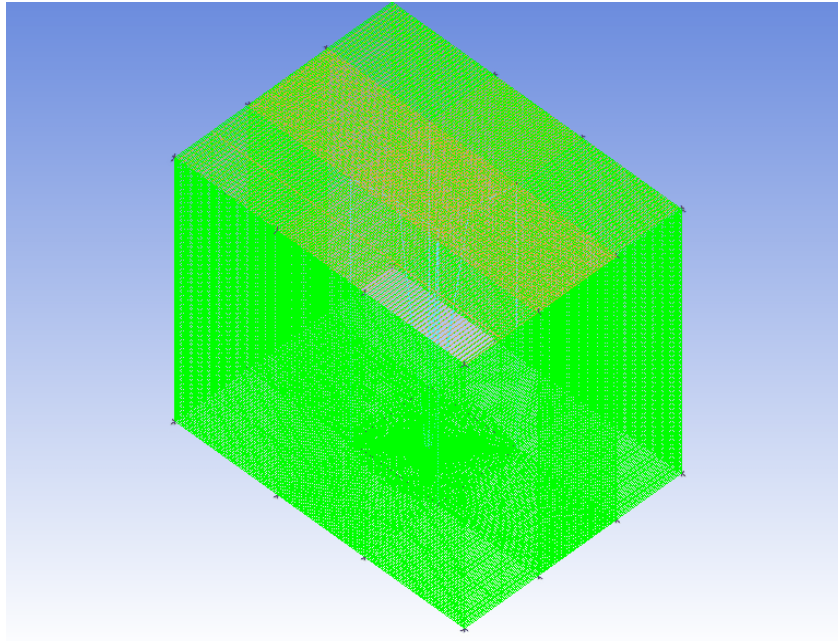
Fig 6.10 ICEM CFD meshing

Meshing is done using ICEM CFD and structured mesh selected in order to capture the physics with good accuracy. The meshing is of a minimum quality of 0.8 (where 0.0 is the worst, 1.0 is the best). The total numbers of elements formed are 1.3 million since it's a complete 3D model. The mesh is deliberately made finer in the center of the geometry since its region of importance. The dimension of the mesh is 1.5x2x1.8 which is convenient to model all the free surfaces at different height required for the simulation.

i. CFD Modelling output

Fig 6.11 : Plume behaviour at
Depth   : 0.5m
Flow Rate : 0.00253m3/s
Radius   :0.0472m
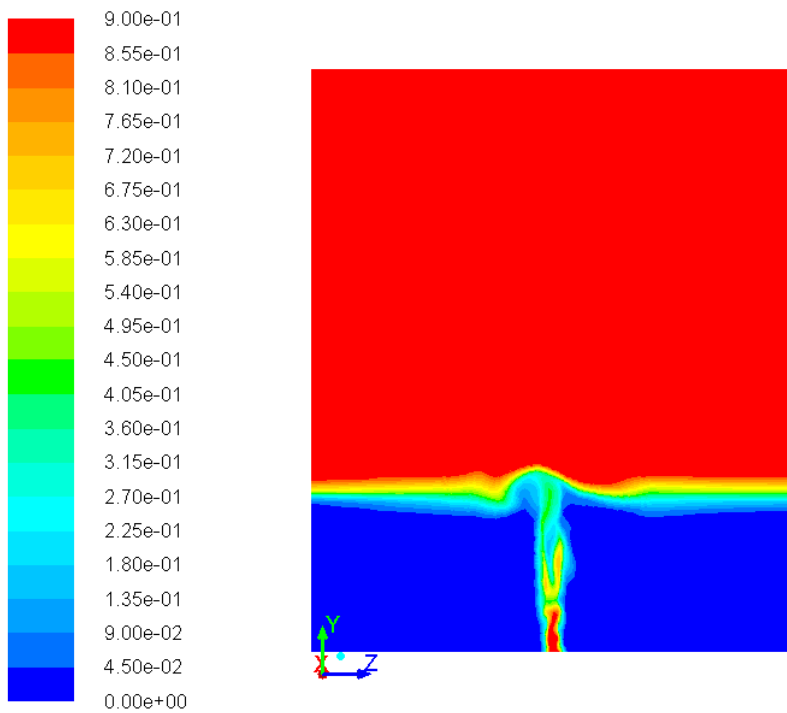
Contours of Volume fraction (air)   (Time=4.9700e+00)

Jun 11, 2013
ANSYS FLUENT 14.0 (3d, pbns, vof, ske, transient)

Fig 6.12 : Plume behaviour at
Depth   : 0.75m
Flow Rate : 0.00505m3/s
Radius   : 0.0726m
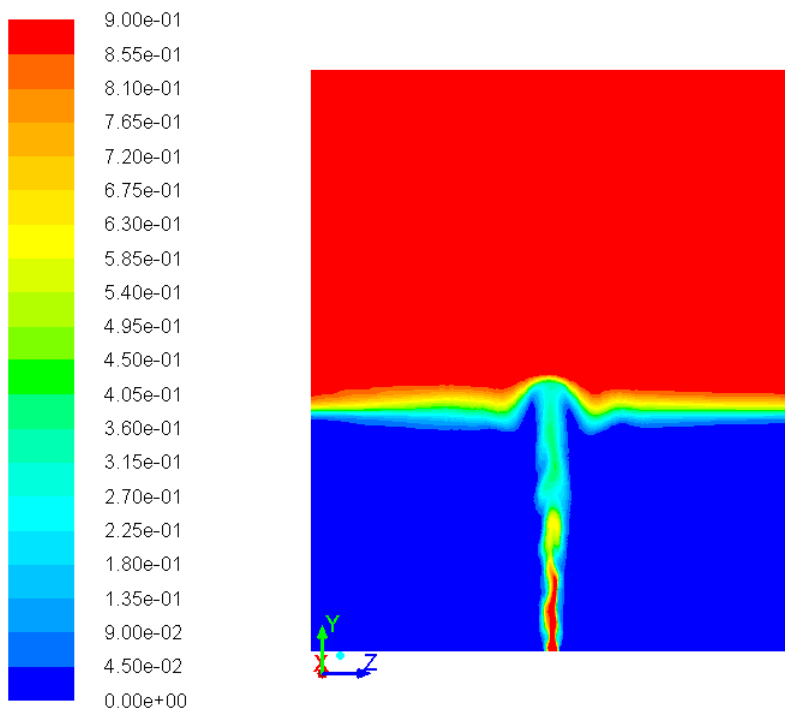
Contours of Volume fraction (air) (Time=3.5900e+00)

Jun 17, 2013
ANSYS FLUENT 14.0 (3d, pbns, vof, ske, transient)

Fig 6.13 : Plume behaviour at
Depth   : 1m
Flow Rate : 0.00758m3/s
Radius   :0.1m
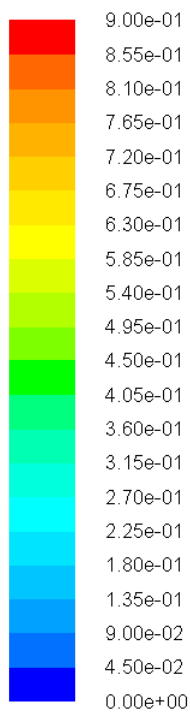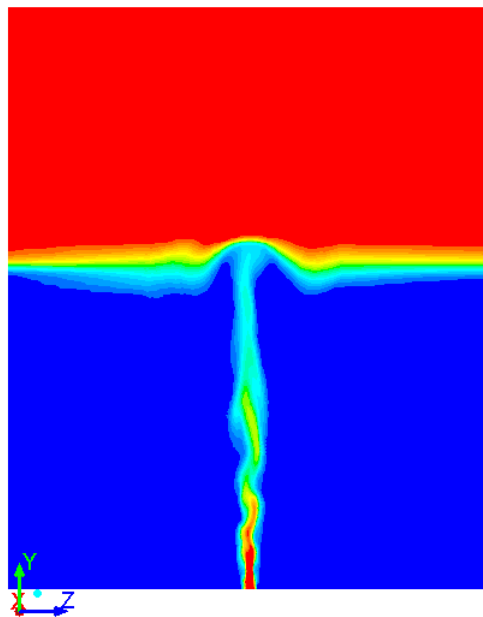
Contours of Volume fraction (air)   (Time=2.9200e+00)   Jun 22, 2013
ANSYS FLUENT 14.0 (3d, pbns, vof, ske, transient)

Fig 6.14 : Plume behaviour at
Depth   : 1.5m
Flow Rate : 0.0112m3/s
Radius   : 0.14m
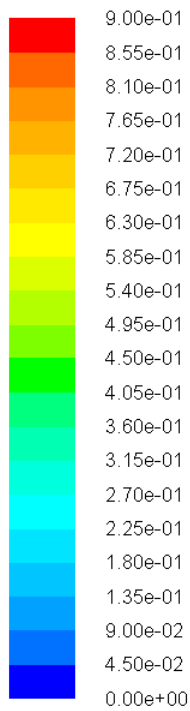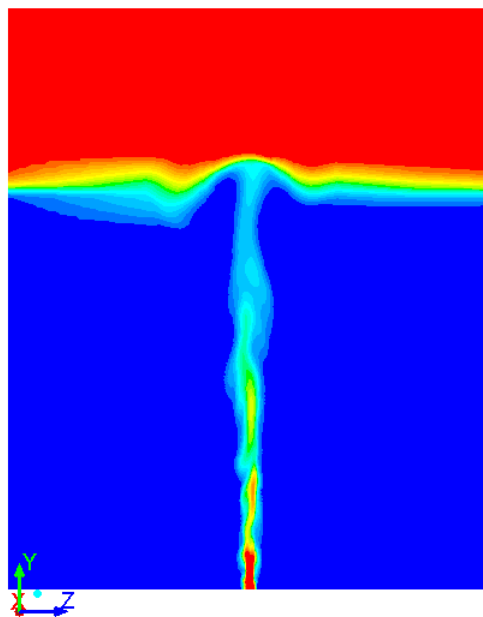
Contours of Volume fraction (air)   (Time=2.9900e+00)

Jul 01, 2013
ANSYS FLUENT 14.0 (3d, pbns, vof, ske, transient)

6.4 Results and inferences from CFD modelling

The results are compared on the basis of quantitative (graphs and values) as well as qualitative approach. The results for all different experimental setups are tabulated and meaningful analogies are drawn.

Table 6.1 ICEM CFD readings

S.N	Ho (m)	Flow rate (m³/s)	Experiment		CFD	
			Radius (m)	Cone Angle	Radius (m)	Cone Angle
1	0.5	0.00253	0.05	11.4212	0.0472	10.78548
2	0.5	0.00505	0.0575	13.1204	0.0498	11.3758
3	0.5	0.00758	0.06	13.6854	0.0558	12.73572
4	0.5	0.0112	0.06	13.6854	0.0612	13.95659
5	0.75	0.00253	0.075	11.4212	0.069	10.51283
6	0.75	0.00505	0.078	11.8748	0.0726	11.05801
7	0.75	0.00758	0.078	11.8748	0.0782	11.90506
8	0.75	0.0112	0.081	12.328	0.0812	12.35831
9	1	0.00253	0.0975	11.1374	0.0916	10.46738
10	1	0.00505	0.0975	11.1374	0.0962	10.98989
11	1	0.00758	0.104	11.8748	0.1002	11.44388
12	1	0.0112	0.104	11.8748	0.1016	11.60269
13	1.5	0.00253	0.132	10.058	0.1094	8.342773
14	1.5	0.00505	0.132	10.058	0.1182	9.011194
15	1.5	0.00758	0.136	10.3612	0.1336	10.17943
16	1.5	0.0112	0.144	10.9672	0.1446	11.0126

Fig 6.15 CFD vs Exp. for Gas flow rate & Plume radius at 0.5m depth

Plume radius (m) vs Gas Flow Rate (kg/s)

- b for H0=0.5m (CFD)
- b for H0=0.5m (Exp.)
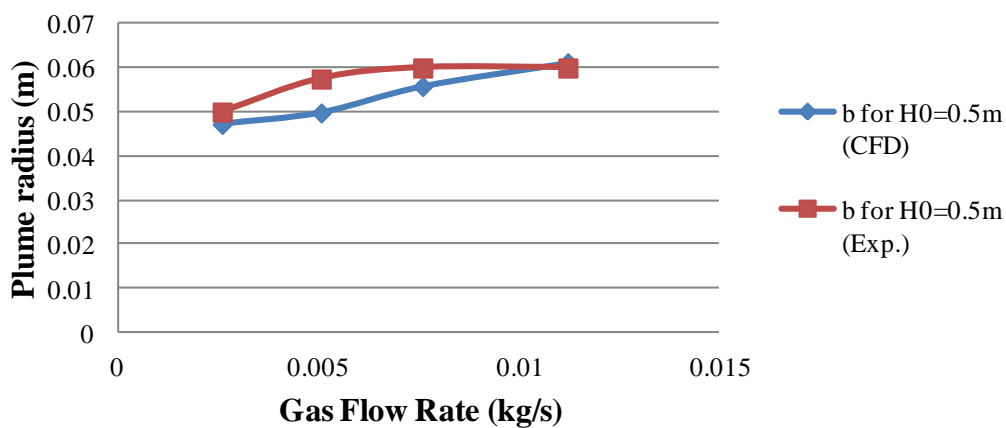
Fig 6.16 CFD vs Exp. for Gas flow rate & Plume radius at 0.75m depth

Plume radius (m) vs Gas Flow Rate (kg/s)

- b for H0=0.75m (CFD)
- b for H0=0.75m (Exp.)
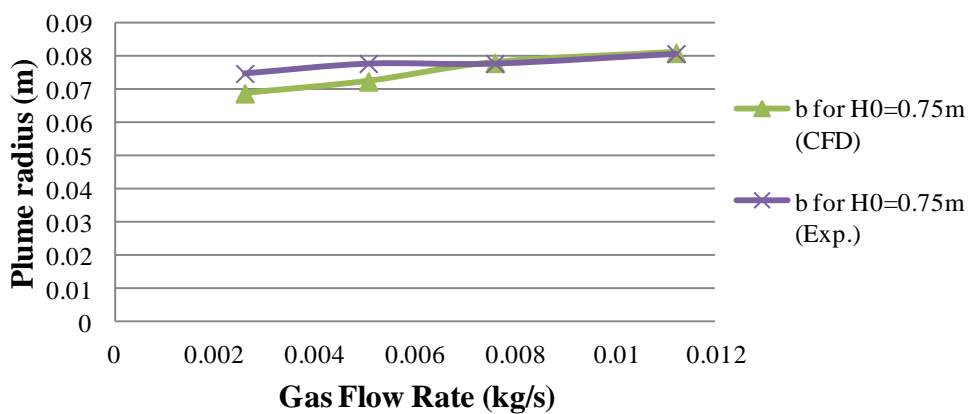
Fig 6.17 CFD vs Exp. for Gas flow rate & Plume radius at 1.0m depth

Plume radius (m) vs Gas Flow Rate (kg/s)

- b for H0=1m(CFD)
- b for H0=1m(Exp.)
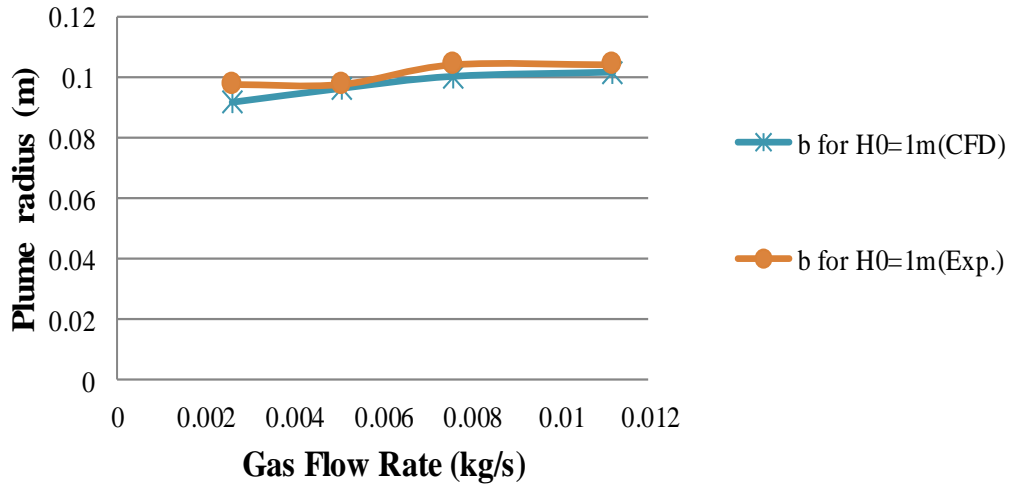
Fig 6.18 CFD vs Exp. for Gas flow rate & Plume radius at 1.5m depth

Plume radius (m) vs Gas Flow Rate (kg/s)

- b for H0=1.5m(CFD)
- b for H0=1.5m(Exp.)

Fig 6.19
CFD vs Exp. for Gas flow rate & Plume radius

Legend:
- b for H0=0.5m (CFD)
- b for H0=0.5m (Exp.)
- b for H0=0.75m (CFD)
- b for H0=0.75m (Exp.)
- b for H0=1m(CFD)
- b for H0=1m (Exp.)
- b for H0=1.5m(CFD)
- b for H0=1.5m(Exp.)

Fig 6.20 CFD vs Exp. for Ocean depth & Plume radius at 0.00258Kg/S

Legend:
- b for Vg=0.00258 (CFD)
- b for Vg=0.00258 (Exp.)
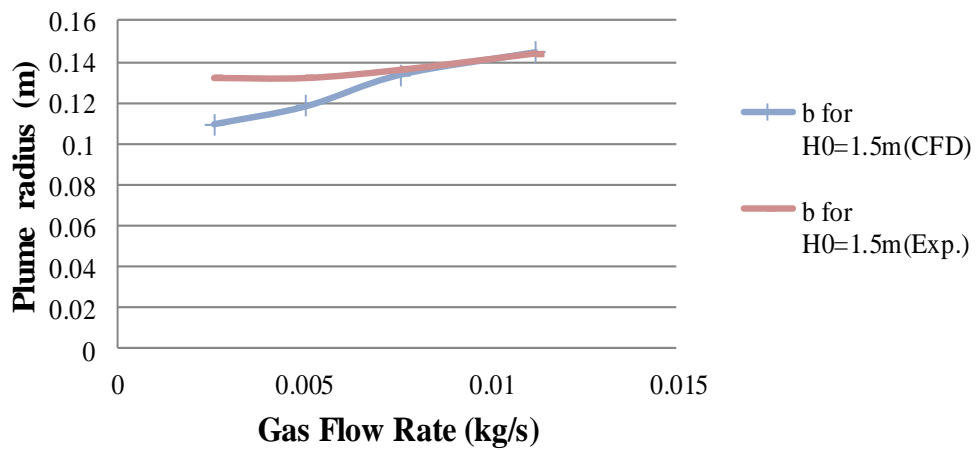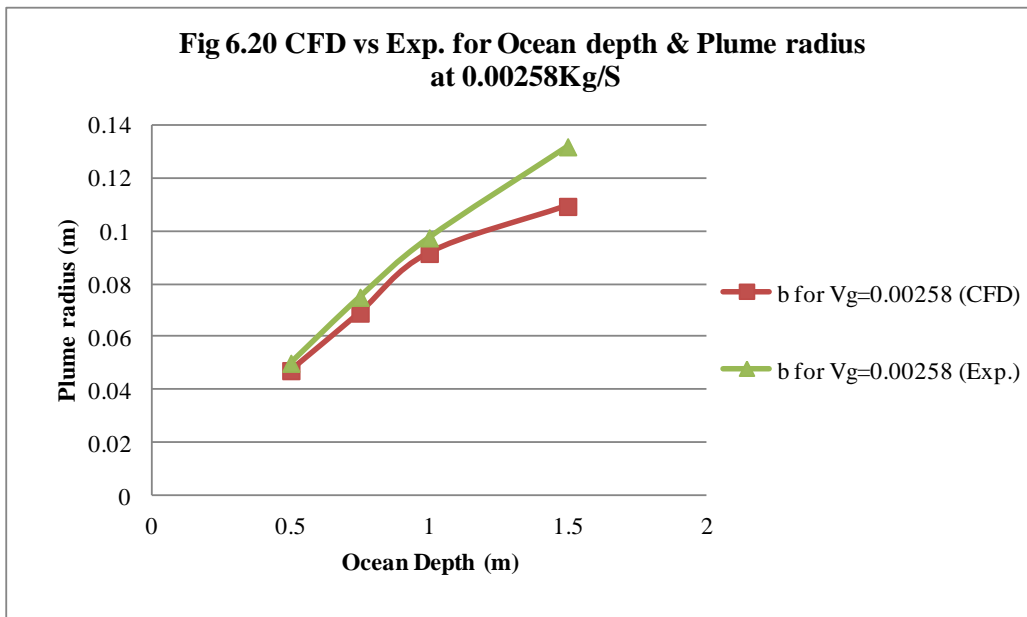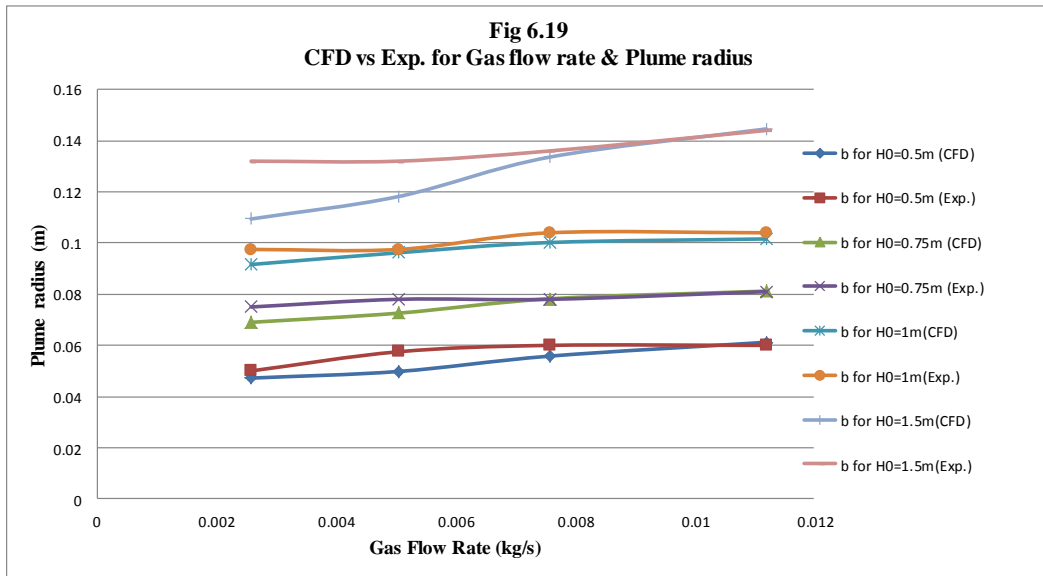
Fig 6.21 CFD vs Exp. for Ocean depth & Plume radius at 0.00505Kg/S
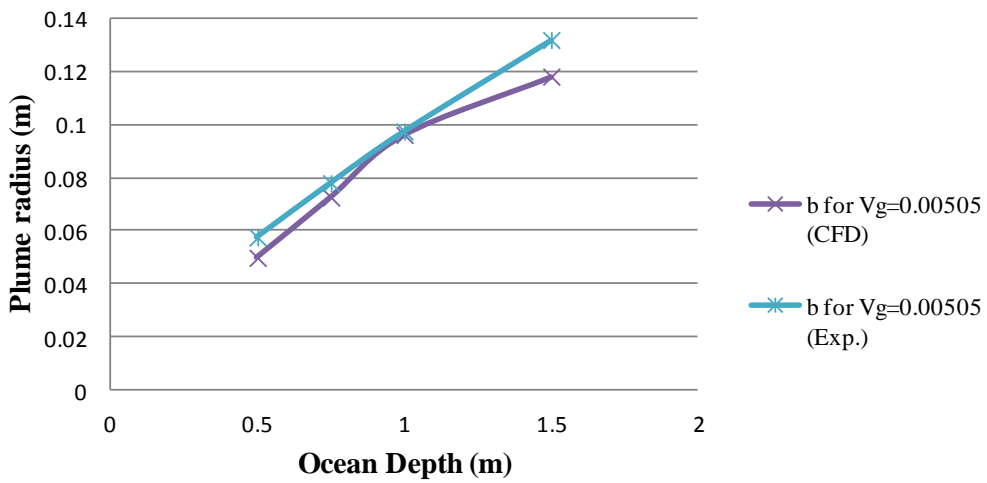
Fig 6.22 CFD vs Exp. for Ocean depth & Plume radius at 0.00758Kg/S
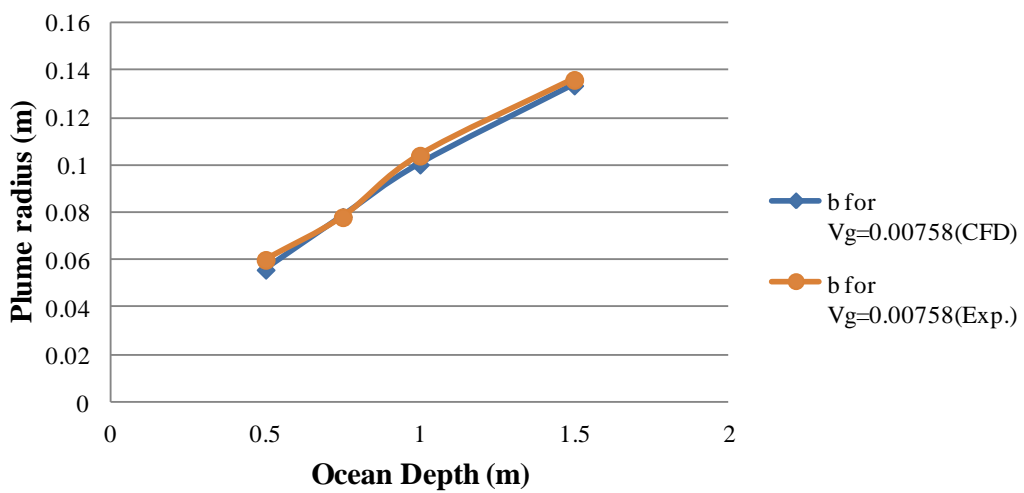
Fig 6.23 CFD vs Exp. for Ocean depth & Plume radius at 0.0112Kg/S
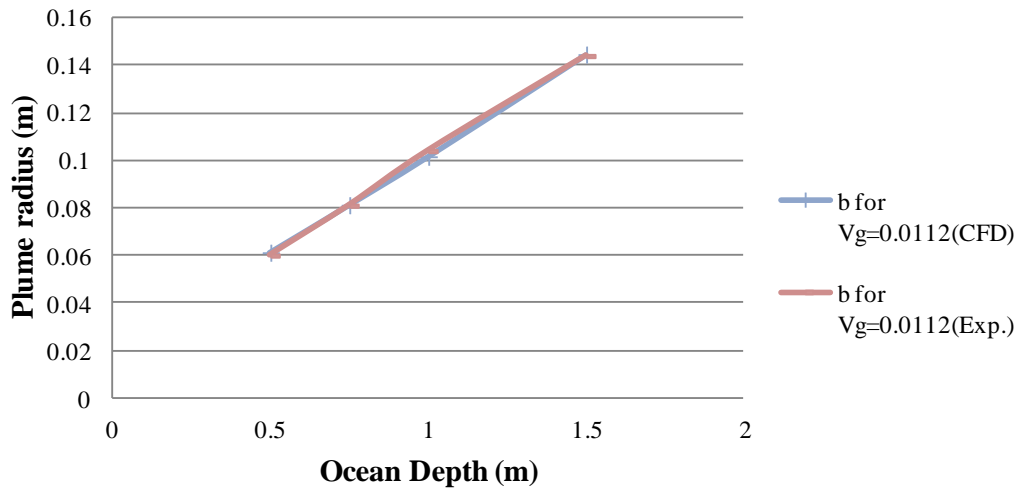
Fig 6.24 CFD vs Exp. for Ocean depth & Plume radius at different flow rates
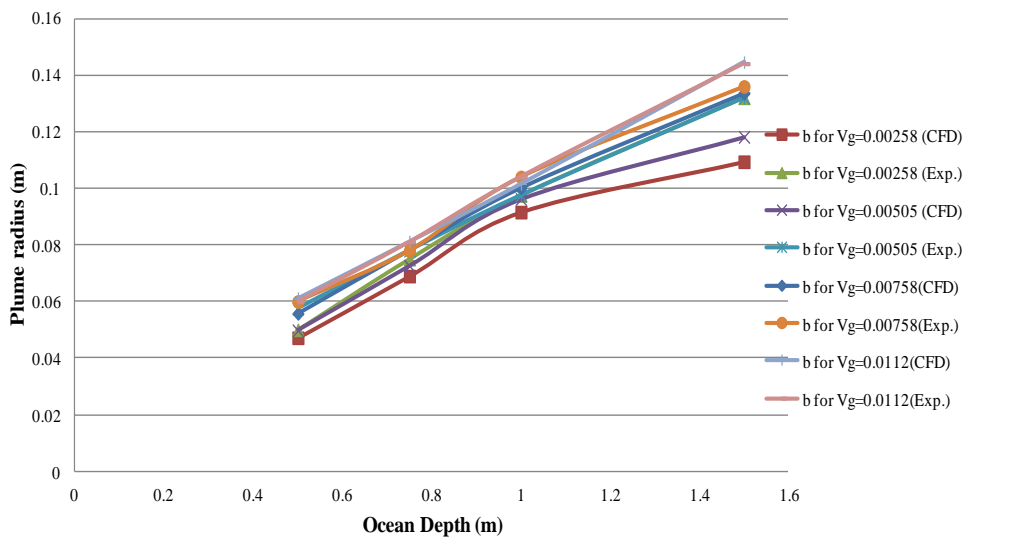
6.5 Chapter summary

6.5.1 Comparison of plume radius and gas flow rates at given depths

Fig. 6.15 to 6.19 shows the comparison of plume radius and gas flow rates at given ocean depths between CFD and experiments.

The trends of CFD and experiments are comparable.

Comparatively CFD trend lines are smoother than experiments trend lines.

At higher flow rates (0.00578Kg/S & 0.0112Kg/S), the radius of the plume is nearly same for both cases (CFD and experiment) as compared to that of lower flow rates for the given depth of the plume.

At lower flow rates, the difference in radius of the plume is comparatively higher in case of experiment than CFD for a given depth and difference decreases with increasing flow rate which is evident from the above graphs (6.15 to 6.19).

At higher depth (1.5m) and lower flow rate (0.00258Kg/s), the difference in radius between CFD and experiment is much greater than compared to smaller depth at same flow rate.

6.5.2 Comparison of plume radius and ocean depth at given flow rates

Fig 6.20 to 6.24 shows the comparison of plume radius and ocean depth at given flow rates between CFD and experiments.

At a given flow rate, the radius at different depths, the CFD and experiment results are observed to be parallel.

The highest difference in radius between CFD and experiment was observed at low flow rate (0.00258Kg/S) and at a depth of 1.5m.

At high flow rate (0.0112Kg/S), the radius at a given ocean depth at respective flow rate are nearly comparable.

In summary, the IIT Experimental results and ICEM CFD outcome are nearly comparable and are corroborated.

7. CONCLUSIONS AND FUTURE RESEARCH

7.1 Chapter overview

This chapter summarises the critical findings, recommendations and conclusions of this research work that includes extensive literature survey, lab-scale experimentation at IIT and ICEM CFD modelling.

7.2 Significance of this research

While the understanding of atmospheric gas dispersion is far advanced, *the need for better understanding of the way hydrocarbon emissions (Plume) behave under water and the risks they present need to greatly improve.* Though limited research is done in UK and in Norway to study the plume behavior for North Sea and Norwegian Sea conditions (< 400 m depth), no such research is done so far in Arabian Sea (for depths ranging from 500m to 1500 m). As the deep water Oil and Gas Exploration and Production will be actively pursued in near future, the need to study the deep-set plume is very essential and hence this research.

The hydrodynamic basis for bubble-plume flows is reasonably well understood, but the solutions of the associated equations, depend on a large number of parameters that can only be evaluated by experimentation.

7.3 Summary of research finding

Lab scale experimentation was carried out at Department of Ocean Engineering, Indian Institute of Technology (IIT), Madras for validating the Empirical/Cone gas discharge plume model established by T.K.Fannelop and M.Bettelini, 2007 [5] for North Sea and Norwegian Sea (i.e.100-400 m depth) for Arabian Sea conditions (i.e. for 500-1500 m depth). The following are key findings of IIT experimentation:

S.N	Parameter varied	Range	Key findings
a.	Water depth Height of water column (Ocean depth)	500 - 1500m	Plume radius marginally increases with water depth.
b.	Leakage/ flow rate/ release rate	0.00253- 0.0112m^3/s	There is less effect of flow rate on plume radius.

c.	Sea temperature	24^0C	Sea temperature does not have any effect on plume behavior.
d.	Salinity	32 – 37 parts per thousand	Salinity does not have any effect on plume behavior.

The plume model established through IIT experimentation for Arabian Sea conditions very well matches with the Plume model established by Fanneløp and Sjøen (1980) [7] and the plume measurements published by Milgram (1983) [17] for North Sea and Norwegian Sea conditions.

The value of the model constants used varies significantly. The cone angle is established as between 10-12°. Lower values closely match that of 10° there by validating the results established by **Wilson, 1988 and Milgram and Erb, 1984** for North Sea and Norwegian Sea.

The 'boil area', where the bubbles break through the surface, has approximately twice the diameter of the bubble plume as determined in the absence of surface interaction. This observation is confirmed by detailed measurements and justifies the use of cone angles even up to 23^0 as established by **Billeter, 1989 and Fanne1op 1989** for North Sea and Norwegian Sea.

7.4 Contributions of this research

In Oil and Gas industry, safety sensitivity studies are undertaken at two levels, relating respectively to consequence modelling and risk assessment. *For consequence modelling, typical release rates and water depths are identified, and, for typical values of these parameters, the above sea consequences are evaluated* for and range of assumptions concerning the interface between the subsea bubble plume and the surface plume or fire.

Higher radius of the plume indicates wider cover area and hence a higher fire and explosion risk. A large area further increases the possibility of coming in contact with the ignition source.

The radius of plume establised by experimentation is in the range of 10-12° which represents low Hazard zone. The IIT Experimental results and ICEM CFD modelling outcome are nearly comparable and are corroborated.

This will help in ascertaining the accuracy of future safety sensitive studies that will be carried out in Arabian Sea for deep sea Exploration & Production (E&P) activities.
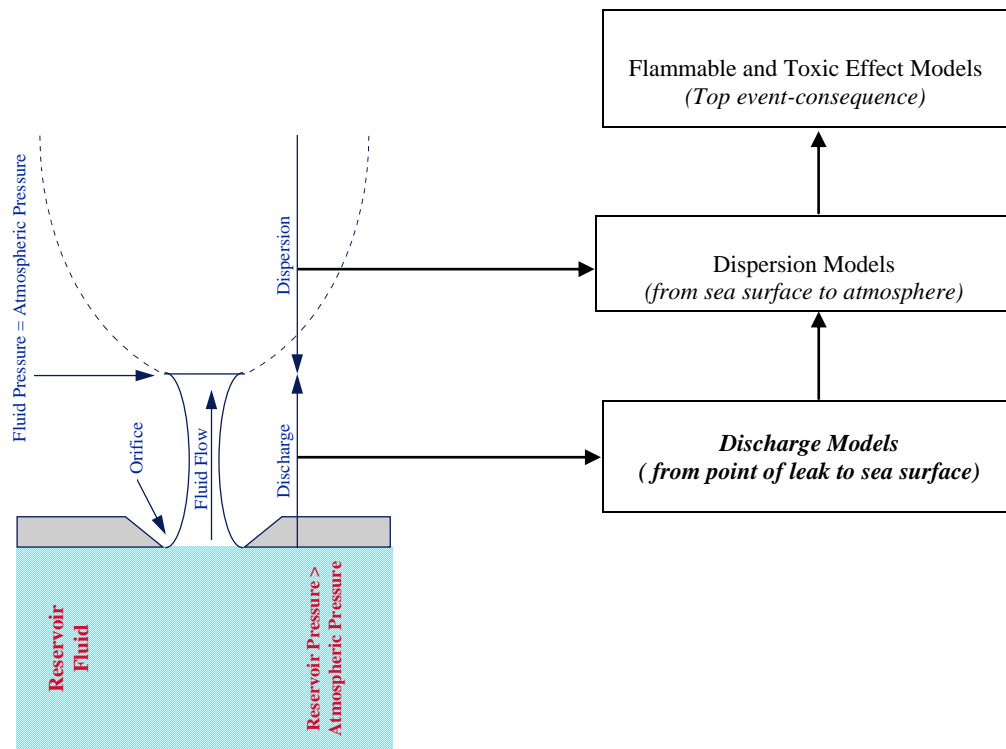
7.5 Limitations and future research

7.5.1 Scaling of experimentation

In the laboratory 10 m appears to be a practical upper limit for the plume depth whereas in offshore applications 50 m to 500 m could be of interest. In recent years a number of laboratory experiments have been conducted with tank depths of the order of 1 m. Most laboratory experiments used gas flow rates of less than 1 kg/s [5]. Source diameter of 1" is chosen based on the real case data available for pipeline failures recorded by HSE Executive, UK. A test tank of 1m depth and shallow water basin of 1.5 m was used for IIT experimentation with the scale down ratio of: 1: 100.

One problem associated with designing suitable experiments is that of scaling-up. For air bubbles rising in a plume in a water tank, the "typical" bubble size will be about 10 mm

regardless of whether the tank is 1 m or 10 m deep. This means the bubble dimension relative to plume (or flow) dimension will not be the same. The bubble size will be largely determined by the surface tension gas-to-water, and it is difficult to tailor this to fit desired scaling relationships. The presence of hydrocarbons in the gas will reduce the surface tension and hence the bubble size, but not enough to make much difference. *For reasons of safety, most laboratory experiments are carried out using air.* For offshore tests, natural gas may be a practical alternative. Momentum loss due to downward and sideward release is not considered. The effect of sea current on plume radius is not taken into account in the experimentation.

7.5.2 Uncertainty of past experiments

The principal sources of uncertainty in the data provided by past experiments and field trials are:

a. the difficulties experienced in measuring fluid phase velocities within a two phase flow using conventional flow meters or laser Doppler anemometry;

b. the difficulty in determining the position of each instrument accurately within the bubble plume;

c. the observation that experimental rigs are themselves subject to movement within the flow;

d. the need to take long time averages of the data, but with little knowledge of the dominant time and length scales of the flow;

e. The use of very low gas flow rates in laboratory scale tests, and flow rates in field trials some two orders of magnitude smaller than that likely for a full scale blow-out;

f. The limited depth of water available in lab-scale tests.

The first three points may be overcome by suitable future design of experiments. The need for more measurements in water depths of 50m and above is also felt necessary. However, the main uncertainty is the lack of any data relating to plume behaviour at realistic release rates. It is currently assumed that the zone of established flow (ZOEF) begins in close proximity to the release source. For high release rates, a substantial part of the subsea plume may actually remain in the zone of flow establishment (ZOFE).

7.5.3 Areas for future research

a. The bubble plume is driven by gas buoyancy. However for higher rates of releases, there may be a significant *jetting length* before buoyancy takes over, and this may be significant compared with the water depth. The jet length and subsequent plume behaviour are a matter of great interest.

b. The effects of *high initial release momentum* or two- phase release on either the plume behaviour or the jetting length is theoretically assumed as approximately equivalent to the Zone of Flow Establishment (ZOFE). This is an interesting area of future research;

c. *Release orientation* should also be considered for large releases. For example, a release directed downward will have its momentum destroyed, and probably behave as a bubble plume, whereas one directed upwards will be more jet- like. Horizontally directed jets would probably result in buoyant plumes offset from the release point by the initial jet throw. This needs to be studied further;

d. In real case, the *drift* of the subsea bubble plume could be significant for deeper waters. This needs to be analysed further!

REFERENCES

1. Bettelini, M.S.G., Fannelop .T.K., 1993, 'Underwater plume from an instantaneously started source', Applied Ocean Research, Vol.15, No.4 pp. 195-206.

2. Billeter L., Fannelop T.K., 1989, 'Gas concentration over an underwater gas release', Atmospheric Environment, Vol.23, issue8, pp. 1683-1694.

3. Ditmars J.D., Cederwall K., 1970, 'Analysis of air bubble plumes', Division of Engineering and Applied Science California Institute of Technology, KH-R-24.

4. Ditmars J.D., Cederwall K., 1974, 'Analysis of Air-Bubble Plumes', Proceedings of the International Conference on Coastal Engineering, No 14, pp. 2209-2226.

5. Fannelop T.K., Bettelini M., 2007, 'Very Large Deep-Set Bubble Plumes From Broken Gas Pipelines', Engineering and Environmental Flow Analysis Asgardstrand.

6. Fannelop T.K., Hirschberg S., Kuffer J., 1991, 'Surface current and recalculating cells generated by bubble curtains and jets', J. Fluid Mechanics, Vol.229 pp. 629-657.

7. Fannelop T.K., Sjoen K., 1980, 'Hydrodynamics of underwater blowouts', Norwegian Maritime Research 4 (1980), pp. 17 -34.

8. Fazal R., Milgram J.H., 1980, 'The structure of gas - liquid plumes above blowout', MIT, Department of Ocean Engg. Report 0380-12.

9. Hasan Abdulmouti, 2011, 'Surface Flow Generation Mechanism Induced by a Bubble Plume', Yanbu Journal of Engineering and Science, Vol.2, ISSN: 1658-5321.

10. Hassan Abdulmouti, Tamer Mohamed Mansour, 2006 'The Technique of PIV and Its Applications' Paper ID ICLASS06-272, Kyoto, Japan.

11. Jan Erik Vinnem, 2007, 'Offshore Risk Assessment, Principles, Modelling and Applications of QRA Studies' 2nd Edition.

12. Loes M., Fannelop T.K., 1989 'Concentration measurements above an underwater release of natural gas', SPE Drilling, June pp. 171-178.

13. McDougall T.J. 1978, 'Bubble plumes in stratified environments', J. Fluid Mechanics, Vol.85, Part 4, pp. 655-672.

14. Milgram J.H., Burgess J.J., 1984, 'Measurement of surface flow above round bubble plume', Massachusetts Inst. of Tech, Cambridge, Applied Ocean Engineering, Vol. 6, No.1, pp. 40-44.

15. Milgram, J. H., Erb, P. R., 1984, 'How Floaters Respond to Subsea Blowouts', Petroleum Engineer, June pp. 64-72.

16. Milgram, J.H., 1982, Van Houten, R.J., 'Plumes from subsea well blowouts', Proceedings of 3rd Tnt. Conf. BOSS. Vol. 1, pp. 659-684.

17. Milgram, J.H., 1983, 'Mean flow in round bubble plumes', J. Fluid Mechanics., Vol.133, pp. 345-376.

18. Morton, B.R., Taylor, G.I. and Turner, J.S. (1956) Turbulent gravitational convection from maintained and instantaneous sources. *Proc. Roy. Soc. A*, **234**, pp 171-178

19. Moros A., Ryall D, 1992, 'Dispersion of flammable gas following a subsea blowout during drilling and its effects on structures', International Gas Research Conference.

20. Moros T, BP Research, Dand I, 1990, 'Two-phase flows as a result of a subsea blowout and their effect on the stability of structures', paper no. OTC 6478, 22nd Annual OTC, Houston, Texas, May.

21. Peng D.Y., Robinson D.B., 1976, 'A New Two-Constant Equation of State'. Ind. Eng. Chem. Fundam., 15, pp. 59-64.

22. Rew P.J, Gallagher P., Deaves D.M., 1995, 'Dispersion of Subsea Releases', Review of Prediction Methodologies, OTH 95 465.

23. Schalk Cloete, Jan Erik Olsen, Paal Skjetne, 2009, 'CFD modeling of plume and free surface behavior resulting from a sub-sea gas release', Applied Ocean Research 31, pp. 220-225.

24. Swan C., Moros A., 1993, 'The hydrodynamics of subsea blowout', Applied Ocean Research, Vol.15 pp. 269-291.

25. Wilson K.J., 1988, 'Effects/Gas-Aerated Seas/Floating Drilling Vessels', Offshore Technology Conference, 2-5 May 1988, Houston, Texas, OTC 5803.

APPENDIX

APPENDIX-A

NOMENCLATURE

b   radius or subsea plume

b(r)   surface current depth as a function of radial coordinate

B(z)   buoyancy force per unit depth

b(z)   radius of sub-sea plume as a function of depth (z)

b_p radius of subsea plume at the surface

c   void fraction

C_D bubble drag coefficient

c_p specific heat capacity at constant pressure of ambient air bubble diameter

c_v specific heat capacity at constant volume of ambient air bubble diameter

D   diameter of flame base (diameter of boil area above the subsea release)

d_b bubble diameter

d_{max} maximum bubble diameter

D_r effective diameter of rupture

f(r,z)   local mean gas fraction

Fi   drag force exerted on the ith bubble

Fr   Froude number

g   acceleration due to gravity

H_B total pressure bead at level of gas release

H_o depth of release

H_T atmospheric pressure head

h_w half depth of surface radial flow

k   fluid turbulent kinetic energy

m   source mass flow rate

M(z)   plume momentum

m_F mass flux of plume at surface

M_F momentum flux of plume at surface

N   number of bubbles per unit volume

p(z)   pressure at height z above sea bed

P_b turbulent kinetic energy generated

q(z)   gas volume flux as a function of water depth

$Q(z)$	volumetric flow rate of the liquid component within the plume
q_t	gas volume flow rate at atmospheric pressure
r	general radial coordinate
r	volume fraction of phase within plume
r_B	radius of the boil area above the subsea release
Re	bubble Reynolds number
$S(z)$	density defect along plume centreline
$S_{F\varnothing}$	source term for phase in transport equations
T_a	ambient temperature
$T_{f\varnothing}$	diffusion coefficient for phase
$U_\varnothing$	velocity vector for phase $\varnothing$
$U(r,z)$	local vertical fluid velocity
$U(z)$	centreline plume velocity as a function of depth (z)
U_b	bubble slip velocity
U_i	component of fluid velocity vector
U_o	initial gas release velocity
V	volume flow rate of entrained air
$V(r,z)$	horizontal plume velocity at surface
V_g	volume flow rate of gas mean surface flow velocity
V_i	instantaneous bubble velocity vector
V_m	mean surface flow velocity
w	centreline velocity
z	Vertical distance from the source (positive towards the surface)
Zo	height of the control volume

Greek

a	plume entrainment coefficient
β	entrainment coefficient for surface flow
ε	turbulent kinetic energy rate of dissipation
λ	ratio of inner gas plume radius to total plume radius
φi	Shape parameters
ϴ	subsea plume cone angle (figure 6.1)
ϒ	momentum amplification factor
Δ	operator representing small but finite change
Δ∨	CFD code cell volume
r_a	density of ambient air
$r_g(o)$	density of gas at source (o)
$r_g(z)$	density of gas at quarter depth (z)
$r_\varnothing$	density of phase in multi-phase flow
$r_p(r,z)$	local mean density within plume density of gas at atmospheric pressure
r_w	mass density of sea-water
ν_t	eddy viscosity
μ	liquid molecular viscosity
∇	gradient operator

INDEX

BIO-DATA OF THE AUTHOR

Sridher is a Mechanical Engineer and a qualified HSE practitioner. He has over 25 years of experience in managing Health, Safety and Environment (HSE), Quality Assurance, Asset Integrity Management (AIMS) and Enterprise-wide Risk Management (ERM) functions in petrochemicals, oil and gas and power industries.

Sridher has presented several technical papers in national and international seminars and conferences. He has also published technical papers in leading magazines and journals. The most recent ones being:

Published papers

- Validating Sub-Sea gas pipeline leaks discharge model for Arabian Sea Conditions, in International Journal of Scientific and Engineering Research (IJSER), Monthly Journal Edition Jan 2013.
- Validating Sub-Sea gas pipeline leaks discharge model for Arabian Sea conditions, in National Safety Council of India (NSCI)'s "Industrial Safety Chronicle" Oct-Dec 2012 issue.

Conference presentations

- Effective management of OH and S in large scale power projects- At National workshop organised by International Finance Corporation (IFC), World Bank Group at New Delhi, Feb 2011.
- "Benchmark Safety Practices", at National Safety Health, and Environment (SHE) Confluence 2012 organised by Dept. of Factories, Boilers, Industrial Safety and Health, Govt. of Karnataka at Bangalore on 04th Mar 2012.
- State level seminar on "Behavioural Based Safety" organized by National Safety Council, Maharashtra chapter, 15th Sep 2012 at Mumbai.
- International Conference on Safety at IIT- Gandhinagar, 14-15th Oct 2012.

Professional memberships

- Member of the National Safety Council of India
- Fellow Member of Safety Engineers Association (India)

CHECK LIST FOR SUBMITTING THE THESIS

The contents of this thesis have the following:

a) Inner cover page;

b) Certificate of the guide(s);

c) Acknowledgements;

d) Executive summary (max 10 pages);

e) Table of contents;

f) List of figures/tables;

g) Body of the thesis;

h) References;

i) Appendices, and;

j) Index;

k) Brief bio-data of the author.

**Submitted to:

Assistant Registrar
University of Petroleum and Energy Studies
Bidholi Campus: Energy Acres, P.O. Bidholi
Via-Prem Nagar
DEHRADUN – 248 007